On the Price of Satisficing in Network User Equilibria

Mahdi Takalloo
Department of Industrial and Management Systems Engineering, University of South Florida, Tampa, FL 33620

Changhyun Kwon*
Department of Industrial and Management Systems Engineering, University of South Florida, Tampa, FL 33620

March 13, 2019

Abstract

When network users are satisficing decision-makers, the resulting traffic pattern attains a satisficing user equilibrium, which may deviate from the (perfectly rational) user equilibrium. In a satisficing user equilibrium traffic pattern, the total system travel time can be worse than in the case of the PRUE. We show how bad the worst-case satisficing user equilibrium traffic pattern can be, compared to the perfectly rational user equilibrium. We call the ratio between the total system travel times of the two traffic patterns the price of satisficing, for which we provide an analytical bound. We compare the analytical bound with numerical bounds for several transportation networks.

Keywords: bounded rationality; satisficing; user equilibrium

1 Introduction

Instead of assuming a perfectly rational person with a clear system of preferences and perfect knowledge of the surrounding decision-making environment, we can consider *boundedly* rational persons with (1) an ambiguous system of preferences and (2) lack of complete information, following Simon (1955). When decision makers are indifferent among alternatives within a certain threshold, they are called *satisficing* decision makers, opposed to *optimizing* decision makers. The notion of satisficing was first introduced by Simon (1955, 1956). Satisficing decision makers choose any alternative whose utility level is above a threshold, called an *aspiration level*, even when the alternative is not optimal. The satisficing behavior is related to the first source of boundedness—an ambiguous system of preferences.

In transportation research, modeling drivers' route choice is an important task. While the travel-time minimization has been traditionally used as a basis for such modeling, sub-optimal route-choice behavior has gained attention. Since Mahmassani and Chang (1987), bounded rationality

*Corresponding author: `chkwon@usf.edu`

has gained attention in the transportation research literature (Szeto and Lo, 2006; Wu et al., 2013; Han et al., 2015; Szeto and Lo, 2006; Ge and Zhou, 2012; Di et al., 2014; Guo, 2013; Lou et al., 2010). Empirical evidence supports bounded rationality of drivers (Nakayama et al., 2001; Zhu and Levinson, 2010). The notion of bounded rationality has also been considered in the evaluation of value of times in connection to route-choice modeling (Xu et al., 2017), and in the model of behavior adjustment process (Ye and Yang, 2017). We refer readers to a review of Di and Liu (2016). In the non-transportation literature, the notion of bounded rationality and satisficing has also received much attention (Charnes and Cooper, 1963; Lam et al., 2013; Jaillet et al., 2016; Chen et al., 1997; Brown and Sim, 2009).

While the above-mentioned transportation research literature considers boundedly rational drivers, their discussion is limited to satisficing drivers without considering the second source of boundedness: lack of complete information on the decision environment. Sun et al. (2018) connect the first and the second sources of boundedness by considering both satisficing behavior and incomplete information, in the context of shortest-path finding in *congestion-free* networks. Sun et al. (2018) study the second source by considering errors in drivers' perception of arc travel time, and conclude that their perception-error model can generally capture both sources of boundedness in rationality in a single unified modeling framework.

In the literature, the traditional network user equilibrium, Wardrop equilibrium in particular, is called the perfectly rational user equilibrium (PRUE), while a traffic pattern equilibrated among satisficing drivers is called a boundedly rational user equilibrium (BRUE). In this paper, we will use a new term *satisficing user equilibrium* (SatUE) instead of BRUE to emphasize that it only considers the first source of boundedness without considering drivers' incomplete information on the decision environment. We believe that the term 'BRUE' should be used to describe a broader and more general class of models, including SatUE.

Note that SatUE differs from the stochastic user equilibrium (SUE) (Sheffi, 1985) in two important aspects. First, drivers are assumed to be optimizing decision makers in SUE, while they are satisficing in SatUE. Second, with appropriate probability distributions assumed in the random utility model in SUE, each path possesses a probability of being chosen; hence we can compute the expected traffic flow rate in each path. In SatUE, however, each satisficing path is acceptable to drivers, but it may or may not be chosen by drivers and we do not know its probability of being chosen. See further discussion in Di and Liu (2016).

The main contribution of this paper is the quantification of how bad the total system travel time in SatUE can be. In a SatUE traffic pattern, the total system travel time can be either greater than or less than that of PRUE. We define the *price of satisficing* (PoSat) as the ratio between the worst-case total system travel time of SatUE and the total system travel time of PRUE. This paper quantifies PoSat analytically and compares with numerical bounds.

The analytical quantification of PoSat is related to the price of anarchy (PoA) (Koutsoupias and Papadimitriou, 1999; Roughgarden and Tardos, 2002) that compares the performances of the system optimal solutions and the PRUE solutions. Using a similar idea, we can also compare the performance of the perfectly rational user equilibrium traffic patterns and satisficing user equilibrium traffic patterns. While PoA quantifies how much system-wide performance we can lose by competing, PoSat quantifies how much we can lose by satisficing. Roughgarden and Tardos (2002) define and study the PoA of *approximate Nash equilibria*, which are essentially SatUE patterns. We develop our bounds for PoSat based on the bounds for PoA of approximate Nash equilibria (Christodoulou et al., 2011) and the ideas from the sensitivity analysis of traffic equilibria (Dafermos and Nagurney, 1984). Note that Perakis (2007) studies the PoA of the *exact* Nash equilibria with general nonlinear, asymmetric cost functions.

The notion of PoSat is also related to the *price of risk aversion* (Nikolova and Stier-Moses, 2015) and the *deviation ratio* (Kleer and Schäfer, 2016). When network users are risk-averse decision makers, the price of risk aversion compares the performances of the resulting equilibrium among risk-averse users and the (risk-neutral) PRUE. When network users' cost functions are deviated from the true cost functions for some reasons, the deviation ratio compares the performances of the resulting equilibrium and the PRUE. Kleer and Schäfer (2016) show that the price of risk aversion is a special case of the deviation ratio. In both research articles, however, only cases with a common single origin node are considered. In this paper, we consider general cases with multiple origin nodes and multiple destination nodes, with asymmetric travel time functions.

This paper is organized as follows. In Section 2, we introduce the notation and define various concepts including user equilibrium, system optimum, satisficing behavior, price of anarchy, and price of satisficing. In Section 3, we define the user equilibrium with perception errors and make connections with satisficing user equilibrium. Our main result is introduced in Section 4, where we derive the analytical worst-case bound on the price of satisficing. In Section 5, we compare the analytical bound with numerical bounds. Section 6 concludes this paper.

2 Notation and Definitions

Since we will use path-based and arc-based flow variables and their corresponding functions and sets interchangeably, we need clear definitions of variables, sets, and functions. We use boldfaced lower-case letters for vector quantities as in $\boldsymbol{v}$ and normal lower-case letters for their components as in v_a; similarly, vector-valued functions like $\boldsymbol{t}(\cdot)$ and their components like $t_a(\cdot)$. We use boldfaced upper-case letters for the set that they belong to, as in $\boldsymbol{v} \in \boldsymbol{V}$. We use calligraphic capital letters for sets of indices as in $\mathcal{N}$. The only exception is a vector $\boldsymbol{Q}$ with Q_w being its elements; we use q_i^w for another value related to Q.

2.1 Traffic Flow Variables and Feasible Sets

We consider a network with a set of origin and destination $\mathcal{W}$ that is represented by directed graph $G(\mathcal{N}, \mathcal{A})$, where $\mathcal{N}$ is the set of nodes, and $\mathcal{A}$ is the set of arcs. For each OD pair $w \in \mathcal{W}$, the travel demand is Q_w and the set of available paths is $\mathcal{P}_w$. The set of all available paths in the whole network is defined as $\mathcal{P} = \cup_{w \in \mathcal{W}} \mathcal{P}_w$.

We also define the set of path flow variables $\boldsymbol{f}$ as

$$\boldsymbol{F} = \left\{ \boldsymbol{f} : \sum_{p \in \mathcal{P}_w} f_p = Q_w \quad \forall w \in \mathcal{W}, \qquad f_p \geq 0 \quad \forall p \in \mathcal{P} \right\}$$

and the corresponding set of arc flow variables $\boldsymbol{v}$ is defined as

$$\boldsymbol{V} = \left\{ \boldsymbol{v} : v_a = \sum_{p \in \mathcal{P}} \delta_a^p f_p \quad \forall a \in \mathcal{A}, \qquad \boldsymbol{f} \in \boldsymbol{F} \right\}$$

where $\delta_a^p = 1$ if path p contains arc a and $\delta_a^p = 0$ otherwise. Let $\mathcal{A}_i^+$ and $\mathcal{A}_i^-$ be the set of arcs whose tail node and head node are i, respectively. When we need to preserve OD information in arc flow variables, we use $\boldsymbol{x}$ as follows:

$$\begin{aligned} \boldsymbol{X} &= \left\{ \boldsymbol{x} : x_a^w = \sum_{p \in \mathcal{P}_w} \delta_a^p f_p \quad \forall a \in \mathcal{A}, w \in \mathcal{W} \qquad \boldsymbol{f} \in \boldsymbol{F} \right\} \\ &= \left\{ \boldsymbol{x} : \sum_{a \in \mathcal{A}_i^+} x_a^w - \sum_{a \in \mathcal{A}_i^-} x_a^w = q_i^w \quad \forall w \in \mathcal{W}, i \in \mathcal{N} \right\} \end{aligned}$$

where $q_i^w = -Q_w$ if $i = o(w)$, $q_i^w = Q_w$ if $i = d(w)$, and $q_i^w = 0$ otherwise.

We have $v_a = \sum_{p \in \mathcal{P}} \delta_a^p f_p$, $x_a^w = \sum_{p \in \mathcal{P}_w} \delta_a^p f_p$, and $v_a = \sum_{w \in \mathcal{W}} x_a^w$. Therefore, the transformations from $\boldsymbol{f}$ to $\boldsymbol{v}$, from $\boldsymbol{f}$ to $\boldsymbol{x}$, and from $\boldsymbol{x}$ to $\boldsymbol{v}$ are unique, which are denoted by $\boldsymbol{f} \mapsto \boldsymbol{v}$, $\boldsymbol{f} \mapsto \boldsymbol{x}$, and $\boldsymbol{x} \mapsto \boldsymbol{v}$, respectively. The inverse transformations are, however, not unique. In the rest of this paper, to emphasize the non-uniqueness of the transformation and refer to *any* result of such transformation, we use $\xrightarrow{\text{any}}$; for example, with $\boldsymbol{v} \xrightarrow{\text{any}} \boldsymbol{f}$, we consider any $\boldsymbol{f}$ such that $v_a = \sum_{p \in \mathcal{P}} \delta_a^p f_p$.

We will use $\boldsymbol{v}$, $\boldsymbol{f}$, and $\boldsymbol{x}$ interchangeably to describe the same traffic pattern. In particular, we define

- $\boldsymbol{f}^*$, $\boldsymbol{v}^*$, $\boldsymbol{x}^*$: system optimal flow vectors (Section 2.2)
- $\boldsymbol{f}^0$, $\boldsymbol{v}^0$, $\boldsymbol{x}^0$: perfectly rational user equilibrium flow vectors (Section 2.3)
- $\boldsymbol{f}^\kappa$, $\boldsymbol{v}^\kappa$, $\boldsymbol{x}^\kappa$: (multiplicative) satisficing user equilibrium flow vectors with κ (Section 2.4)

Note that when $\kappa = 0$, we have $\boldsymbol{f}^\kappa = \boldsymbol{f}^0$.

2.2 Travel Time Functions and System Optimum

We denote arc travel function with arc traffic volume $\boldsymbol{v}$ by $t_a(\boldsymbol{v})$ for each arc $a \in \mathcal{A}$. We consider a performance function for each arc a as

$$z_a(\boldsymbol{v}) = t_a(\boldsymbol{v}) v_a.$$

We denote the travel time function along path p with flow $\boldsymbol{f}$ by $c_p(\boldsymbol{f})$. When problems are stated with respect to $\boldsymbol{x}$, given $v_a = \sum_w x_a^w$, we define $\tau_a^w(\boldsymbol{x}) = \tau_a(\boldsymbol{x}) = t_a(\boldsymbol{v})$. We can consider path-based performance function as follows

$$z_p(\boldsymbol{f}) = c_p(\boldsymbol{f}) f_p.$$

Arc travel function and flow travel function are related to each other:

$$c_p(\boldsymbol{f}) = \sum_{a \in \mathcal{A}} \delta_a^p t_a(\boldsymbol{v}).$$

We define the arc-based total system performance function $Z(\boldsymbol{v})$ and path-based total system performance function $C(\boldsymbol{f})$ interchangeably as follows:

$$\begin{aligned} Z(\boldsymbol{v}) &\equiv \sum_{a \in \mathcal{A}} z_a(\boldsymbol{v}) = \sum_{a \in \mathcal{A}} t_a(\boldsymbol{v}) v_a \\ &= \sum_{p \in \mathcal{P}} z_p(\boldsymbol{f}) = \sum_{p \in \mathcal{P}} c_p(\boldsymbol{f}) f_p = \sum_{w \in \mathcal{W}} \sum_{p \in \mathcal{P}_w} c_p(\boldsymbol{f}) f_p \equiv C(\boldsymbol{f}), \end{aligned}$$

which is also called the total system travel time. A flow pattern that minimizes $Z(\cdot)$ or $C(\cdot)$ is called a *system optimal* flow pattern.

The vector-valued function $\boldsymbol{t}(\cdot)$ is called *monotone* in $\boldsymbol{V}$ if

$$[\boldsymbol{t}(\boldsymbol{v}^1) - \boldsymbol{t}(\boldsymbol{v}^2)]^\top (\boldsymbol{v}^1 - \boldsymbol{v}^2) \geq 0 \tag{1}$$

for all $\boldsymbol{v}^1, \boldsymbol{v}^2 \in \boldsymbol{V}$. If (1) holds as a strict inequality for all $\boldsymbol{v}^1 \neq \boldsymbol{v}^2$, it is said *strictly monotone*. The function $\boldsymbol{t}(\cdot)$ is called *strongly monotone* in $\boldsymbol{V}$ with modulus $\alpha > 0$ if

$$[\boldsymbol{t}(\boldsymbol{v}^1) - \boldsymbol{t}(\boldsymbol{v}^2)]^\top (\boldsymbol{v}^1 - \boldsymbol{v}^2) \geq \alpha \left\| \boldsymbol{v}^1 - \boldsymbol{v}^2 \right\|_{\boldsymbol{V}}^2 \tag{2}$$

for all $\boldsymbol{v}^1, \boldsymbol{v}^2 \in \boldsymbol{V}$, where $\|\cdot\|_{\boldsymbol{V}}$ is the l^2-norm in $\boldsymbol{V}$. The monotonicity of path-based travel time function $c_p(\cdot)$ or its vector form $\boldsymbol{c}(\cdot)$ can be similarly defined. The path-based function $c_p(\cdot)$, however, is not strongly monotone in general (e.g., see Example 3 in de Palma and Nesterov, 1998).

2.3 Perfectly Rational User Equilibrium

When network users are perfectly rational, i.e. they seek the shortest path, we attain the perfectly rational user equilibrium (PRUE) defined as follows:

Definition 1 (Perfectly Rational User Equilibrium)**.** A traffic pattern $\boldsymbol{f}^0$ is called a *perfectly rational user equilibrium* (PRUE), if

$$(\mathsf{PRUE}) \qquad f_p^0 > 0 \implies c_p(\boldsymbol{f}^0) = \min_{p' \in \mathcal{P}_w} c_{p'}(\boldsymbol{f}^0) \tag{3}$$

for all $p \in \mathcal{P}_w$ and $w \in \mathcal{W}$.

Using the arc travel function, the above condition can be restated as follows

$$f_p^0 > 0 \implies \sum_{a \in \mathcal{A}} \delta_a^p t_a(\boldsymbol{v}^0) = \min_{p' \in \mathcal{P}_w} \sum_{a \in \mathcal{A}} \delta_a^{p'} t_a(\boldsymbol{v}^0) \tag{4}$$

for all $p \in \mathcal{P}_w$ and $w \in \mathcal{W}$.

It is well known that a solution to the following variational inequality problem is a user equilibrium traffic flow (Smith, 1979; Dafermos, 1980):

$$\text{to find } \bar{\boldsymbol{f}} \in \boldsymbol{F} : \sum_{p \in \mathcal{P}} c_p(\bar{\boldsymbol{f}})(f_p - \bar{f}_p) \geq 0 \qquad \forall \boldsymbol{f} \in \boldsymbol{F}, \tag{5}$$

which can be equivalently rewritten as:

$$\text{to find } \bar{\boldsymbol{v}} \in \boldsymbol{V} : \sum_{a \in \mathcal{A}} t_a(\bar{\boldsymbol{v}})(v_a - \bar{v}_a) \geq 0 \qquad \forall \boldsymbol{v} \in \boldsymbol{V}, \tag{6}$$

or

$$\text{to find } \bar{\boldsymbol{x}} \in \boldsymbol{X} : \sum_{a \in \mathcal{A}} \sum_{w \in \mathcal{W}} \tau_a(\bar{\boldsymbol{x}})(x_a^w - \bar{x}_a^w) \geq 0 \qquad \forall \boldsymbol{x} \in \boldsymbol{X} \tag{7}$$

where $\tau_a^w(\boldsymbol{x}) = \tau_a(\boldsymbol{x}) = t_a(\boldsymbol{v})$.

With strictly monotone functions $t_a(\cdot)$, the solution $\bar{\boldsymbol{v}}$ to (6) is unique. While the transformations $\bar{\boldsymbol{v}} \overset{\text{any}}{\longmapsto} \bar{\boldsymbol{f}}$ and $\bar{\boldsymbol{v}} \overset{\text{any}}{\longmapsto} \bar{\boldsymbol{x}}$ are not unique, any such $\bar{\boldsymbol{f}}$ and $\bar{\boldsymbol{x}}$ are solutions to (5) and (7), respectively; therefore, solutions to (5) and (7) are not unique in general.

When the travel time on arc a is a function of only v_a, i.e. $t_a = t_a(v_a)$, then it is called *separable*. With separable arc travel time functions, the variational inequality problem (6) admits an equivalent convex optimization problem as formulated by (Beckmann et al., 1956). In general, if the Jacobian matrix of the arc travel time function vector $\boldsymbol{t}(\boldsymbol{v})$ is symmetric, that is,

$$\frac{\partial t_a(\boldsymbol{v})}{\partial v_e} = \frac{\partial t_e(\boldsymbol{v})}{\partial v_a} \qquad \forall a, e \in \mathcal{A},$$

for all $\boldsymbol{v} \in \boldsymbol{V}$, the variational inequality problem (6) can be reformulated as such an equivalent Beckmann-type convex optimization problem (Patriksson, 2015; Friesz and Bernstein, 2016). When the Jacobian is asymmetric, we cannot reformulate (6) as a Beckmann-type convex optimization problem in general; in which case, we call the arc travel time functions *asymmetric* and we work with the variational inequality form (6) to find and analyze PRUE.

2.4 Satisficing User Equilibrium

We introduce definitions of satisficing behavior and corresponding user equilibrium traffic patterns. A typical definition in the transportation research literature (e.g. Lou et al., 2010; Di et al., 2013; Han et al., 2015), termed boundedly rational user equilibrium (BRUE), uses an additive term. We call it additive satisficing user equilibrium, since bounded rationality could imply a broader concept than just satisficing behavior.

Definition 2 (Additive Satisficing)**.** A traffic pattern $\boldsymbol{f}$ is called an *additive satisficing user equilibrium (ASatUE)* with E, if

$$(\mathsf{ASatUE}) \qquad f_p > 0 \implies c_p(\boldsymbol{f}) \leq \min_{p' \in \mathcal{P}_w} c_{p'}(\boldsymbol{f}) + E \tag{8}$$

for all $p \in \mathcal{P}_w$ and $w \in \mathcal{W}$, where E is a positive constant.

We can also derive a similar definition using a multiplicative term. While the additive form in Definition 2 is popularly used in the transportation research literature, the multiplicative form in Definition 3 enables us to consider the satisficing level in disaggregate arc levels as we will observe in this paper. Multiplicative satisficing user equilibrium is also called approximate Nash equilibrium in the price of anarchy literature (Christodoulou et al., 2011).

Definition 3 (Multiplicative Satisficing)**.** A traffic pattern $\boldsymbol{f}^\kappa$ is called a *multiplicative satisficing user equilibrium* with κ, or κ-MSatUE, if

$$(\mathsf{MSatUE}) \qquad f_p^\kappa > 0 \implies c_p(\boldsymbol{f}^\kappa) \leq (1+\kappa) \min_{p' \in \mathcal{P}_w} c_{p'}(\boldsymbol{f}^\kappa) \tag{9}$$

for all $p \in \mathcal{P}_w$ and $w \in \mathcal{W}$, where $\kappa \geq 0$ is a constant.

Note that E in (8) and κ in (9) may be defined for each OD pair w, for example E_w and κ_w respectively, to allow non-homogeneous satisficing threshold for each OD pair w. In such cases, however, we assume that travelers for the same OD pair are homogeneous with the same threshold κ_w. In this paper, for simplicity, we use a single value of κ for all OD pairs.

2.5 Price of Satisficing

The price of anarchy (PoA) compares the performances of approximate Nash equilibrium and system optimum; $C(\boldsymbol{f}^\kappa)$ and $C(\boldsymbol{f}^*)$, respectively. Among possibly multiple approximate Nash equilibrium traffic patterns, we are interested in the worst-case. We let the tuple $(G, \boldsymbol{Q}, \boldsymbol{t})$ denote a problem instance for any given κ. Let us denote the set of approximate Nash equilibrium for a given problem instance by $\Psi_\kappa(G, \boldsymbol{Q}, \boldsymbol{t})$. We can define PoA of the problem instance $(G, \boldsymbol{Q}, \boldsymbol{t})$ as follows:

$$\mathsf{PoA}_\kappa(G, \boldsymbol{Q}, \boldsymbol{t}) = \max_{\boldsymbol{f}^\kappa \in \Psi_\kappa(G, \boldsymbol{Q}, \boldsymbol{t})} \frac{C(\boldsymbol{f}^\kappa)}{C(\boldsymbol{f}^*)}, \tag{10}$$

where $\boldsymbol{f}^*$ is the system optimum flow for $(G, \boldsymbol{Q}, \boldsymbol{t})$. We are usually interested in its upper bound

$$\sup_{(G, \boldsymbol{Q}, \boldsymbol{t}) \in \Omega} \mathsf{PoA}_\kappa(G, \boldsymbol{Q}, \boldsymbol{t})$$

for a family of instances Ω.

In the context of bounded rationality and satisficing, we are more interested in comparing the performance of approximate Nash equilibrium $C(\boldsymbol{f}^\kappa)$ and the performance of the perfectly rational user equilibrium $C(\boldsymbol{f}^0)$. We define the price of satisifcing (PoSat) of instance $(G, \boldsymbol{Q}, \boldsymbol{t})$ as follows:

$$\mathsf{PoSat}_\kappa(G, \boldsymbol{Q}, \boldsymbol{t}) = \max_{\boldsymbol{f}^\kappa \in \Psi_\kappa(G, \boldsymbol{Q}, \boldsymbol{t})} \frac{C(\boldsymbol{f}^\kappa)}{C(\boldsymbol{f}^0)}, \tag{11}$$

and its upper bound

$$\sup_{(G, \boldsymbol{Q}, \boldsymbol{t}) \in \Omega} \mathsf{PoSat}_\kappa(G, \boldsymbol{Q}, \boldsymbol{t})$$

for a family of instance Ω. In this paper, we are interested in a family of instances where G is a directed graph, $\boldsymbol{Q}$ are constants, and $\boldsymbol{t}(\cdot)$ is a polynomial function of order n. We let $\Omega(n)$ be such a family for any $n \geq 0$.

3 User Equilibrium with Perception Errors

Related to MSatUE, we introduce the user equilibrium with perception error (UE-PE) model. In this model, we assume that network users are optimizing, i.e. seeking the shortest path; however, we assume that users may have their own perception of the travel time function.

We let ε_a^w denote the perception error of travel time along arc a of users in OD pair w. A vector $\bar{\boldsymbol{x}} \in \boldsymbol{X}$ is a solution to the UE-PE model, if

$$\sum_{a \in \mathcal{A}} \sum_{w \in \mathcal{W}} (t_a(\bar{\boldsymbol{v}}) - \varepsilon_a^w)(x_a^w - \bar{x}_a^w) \geq 0 \qquad \forall \boldsymbol{x} \in \boldsymbol{X} \tag{12}$$

for *some* $\boldsymbol{\varepsilon}$ such that $\varepsilon_a^w \leq t_a(\bar{\boldsymbol{v}})$ for all $a \in \mathcal{A}, w \in \mathcal{W}$. We note that $t_a(\bar{\boldsymbol{v}}) - \varepsilon_a^w$ is the *perceived* travel time for drivers of OD pair w. The term ε_a^w represents the perception error for arc a and OD pair w. In this model, we assume all drivers for each OD pair are homogeneous in their perception of arc travel time.

With changes of variables $\lambda_a^w t_a(\boldsymbol{v}) = t_a(\boldsymbol{v}) - \varepsilon_a^w$, the UE-PE model (12) can be restated as follows:

$$(\mathsf{UE\text{-}PE\text{-}}\boldsymbol{X}) \qquad \sum_{a \in \mathcal{A}} \sum_{w \in \mathcal{W}} \lambda_a^w t_a(\bar{\boldsymbol{v}})(x_a^w - \bar{x}_a^w) \geq 0 \qquad \forall \boldsymbol{x} \in \boldsymbol{X} \tag{13}$$

for some $\boldsymbol{\lambda}$ such that $\lambda_a^w \geq 0$ for all $w \in \mathcal{W}$ and $a \in \mathcal{A}$. We observe that the UE-PE model generates a subset of MSatUE traffic flow patterns.

Lemma 1 ($\mathsf{UE\text{-}PE\text{-}}\boldsymbol{X} \implies$ MSatUE)**.** *Suppose $\bar{\boldsymbol{x}}$ is a solution to* $\mathsf{UE\text{-}PE\text{-}}\boldsymbol{X}$ *in* (13) *with some $\bar{\boldsymbol{\lambda}}$ where $\bar{\lambda}_a^w \in [\frac{1}{1+\kappa}, 1]$ for all $w \in \mathcal{W}$ and $a \in \mathcal{A}$. Then any $\bar{\boldsymbol{f}}$ with $\bar{\boldsymbol{x}} \overset{\text{any}}{\longmapsto} \bar{\boldsymbol{f}}$ is a κ-MSatUE flow.*

Proof of Lemma 1. Given $\bar{\boldsymbol{f}}$, we let $\bar{\boldsymbol{v}}$ be the arc flow vector from $\bar{\boldsymbol{f}} \mapsto \bar{\boldsymbol{v}}$. Let $\bar{\varepsilon}$ is the perception error that makes $\bar{\boldsymbol{x}}$ a solution to (12). Under the perception error $\bar{\varepsilon}$, we know that $\bar{\boldsymbol{x}}$ is a user equilibrium traffic flow; hence the following condition holds from (4):

$$\bar{f}_p > 0 \implies \sum_{a\in\mathcal{A}} \delta_a^p \bar{\lambda}_a^w t_a(\bar{\boldsymbol{v}}) = \min_{p'\in\mathcal{P}_w} \sum_{a\in\mathcal{A}} \delta_a^{p'} \bar{\lambda}_a^w t_a(\bar{\boldsymbol{v}}) \tag{14}$$

for all $p \in \mathcal{P}_w$ and $w \in \mathcal{W}$. Since $\bar{\lambda}_a^w \in [\frac{1}{1+\kappa}, 1]$, the right-hand-side of (14) implies

$$\frac{1}{1+\kappa} \sum_{a\in\mathcal{A}} \delta_a^p t_a(\bar{\boldsymbol{v}}) \leq \min_{p'\in\mathcal{P}_w} \sum_{a\in\mathcal{A}} \delta_a^{p'} \bar{\lambda}_a^w t_a(\bar{\boldsymbol{v}}) \leq \min_{p'\in\mathcal{P}_w} \sum_{a\in\mathcal{A}} \delta_a^{p'} t_a(\bar{\boldsymbol{v}}),$$

which is equivalent to the following path flow form:

$$c_p(\bar{\boldsymbol{f}}) \leq (1+\kappa) \min_{p'\in\mathcal{P}_w} c_{p'}(\bar{\boldsymbol{f}}).$$

Therefore, we conclude that $\bar{\boldsymbol{f}}$ is a κ-MSatUE traffic flow. □

We can also provide a path-based formulation of UE-PE:

$$(\textsf{UE-PE-}\boldsymbol{F}) \qquad \sum_{w\in\mathcal{W}} \sum_{p\in\mathcal{P}_w} \widetilde{c}_p^w(\bar{\boldsymbol{f}})(f_p - \bar{f}_p) \geq 0 \qquad \forall \boldsymbol{f} \in \boldsymbol{F} \tag{15}$$

for the perceived path travel time functions $\widetilde{c}_p^w(\boldsymbol{f}) = \sum_{a\in\mathcal{A}} \delta_a^p \lambda_a^w t_a(\boldsymbol{v})$ with *some* $\boldsymbol{\lambda}$ such that $\lambda_a^w \geq 0$ for all $a \in \mathcal{A}, w \in \mathcal{W}$.

Lemma 2 (UE-PE-$\boldsymbol{F}$ $\iff$ UE-PE-$\boldsymbol{X}$)**.** *If $\bar{\boldsymbol{f}} \in \boldsymbol{F}$ is a solution to* UE-PE-$\boldsymbol{F}$ *in* (15) *for some $\boldsymbol{\lambda}$ such that $\lambda_a^w \in [\frac{1}{1+\kappa}, 1]$, then $\bar{\boldsymbol{x}}$ with $\bar{\boldsymbol{f}} \mapsto \bar{\boldsymbol{x}}$ is a solution to* UE-PE-$\boldsymbol{X}$ *in* (13)*. Conversely, if $\bar{\boldsymbol{x}} \in \boldsymbol{X}$ is a solution to* UE-PE-$\boldsymbol{X}$ *in* (13)*, then any $\bar{\boldsymbol{f}}$ with $\bar{\boldsymbol{x}} \overset{\text{any}}{\longmapsto} \bar{\boldsymbol{f}}$ is a solution to* UE-PE-$\boldsymbol{F}$ *in* (15)*.*

Proof of Lemma 2. We can prove both directions by observing that

$$\begin{aligned}
\sum_{w\in\mathcal{W}} \sum_{p\in\mathcal{P}_w} \widetilde{c}_p^w(\bar{\boldsymbol{f}})(f_p - \bar{f}_p) &= \sum_{w\in\mathcal{W}} \sum_{p\in\mathcal{P}_w} \sum_{a\in\mathcal{A}} \delta_a^p \lambda_a^w t_a(\bar{\boldsymbol{v}})(f_p - \bar{f}_p) \\
&= \sum_{w\in\mathcal{W}} \sum_{a\in\mathcal{A}} \lambda_a^w t_a(\bar{\boldsymbol{v}}) \Bigg(\sum_{p\in\mathcal{P}_w} \delta_a^p f_p - \sum_{p\in\mathcal{P}_w} \delta_a^p \bar{f}_p \Bigg) \\
&= \sum_{w\in\mathcal{W}} \sum_{a\in\mathcal{A}} \lambda_a^w t_a(\bar{\boldsymbol{v}})(x_a^w - \bar{x}_a^w).
\end{aligned}$$

□

When the values of λ_a^w are the same across all $w \in \mathcal{W}$, i.e. $\lambda_a = \lambda_a^w$ for all $w \in \mathcal{W}$, we can simplify (13) as follows:

$$(\textsf{UE-PE-}\boldsymbol{V}) \qquad \sum_{a\in\mathcal{A}} \lambda_a t_a(\bar{\boldsymbol{v}})(v_a - \bar{v}_a) \geq 0 \qquad \forall \boldsymbol{v} \in \boldsymbol{V} \tag{16}$$

$$\mathsf{UE\text{-}PE\text{-}}\boldsymbol{V} \Longrightarrow \mathsf{UE\text{-}PE\text{-}}\boldsymbol{X} \Longrightarrow \text{MSatUE} \Longrightarrow (17)$$

$$\Updownarrow$$

$$\mathsf{UE\text{-}PE\text{-}}\boldsymbol{F}$$

Figure 1: Summary of Lemmas 1–4. The relation $\mathsf{X} \implies \mathsf{Y}$ means that any solution to X yields a solution to Y.

for *some* $\boldsymbol{\lambda}$ such that $\lambda_a \geq 0$ for each $a \in \mathcal{A}$. The simplified model (16) has been considered in the literature for approximate Nash equilibrium (Christodoulou et al., 2011) and Nash equilibrium with deviated travel time functions (Kleer and Schäfer, 2016). For the simplified model, we can state:

Lemma 3 ($\mathsf{UE\text{-}PE\text{-}}\boldsymbol{V} \implies \mathsf{UE\text{-}PE\text{-}}\boldsymbol{X}$)**.** *Suppose that $\bar{v} \in \boldsymbol{V}$ is a solution to* $\mathsf{UE\text{-}PE\text{-}}\boldsymbol{V}$ *in* (16) *for some $\boldsymbol{\lambda}$ such that $\lambda_a \in [\frac{1}{1+\kappa}, 1]$ for all $a \in \mathcal{A}$. Let $\bar{\boldsymbol{x}}$ be any vector with $\bar{\boldsymbol{v}} \overset{\text{any}}{\longmapsto} \bar{\boldsymbol{x}}$. Then $\bar{\boldsymbol{x}}$ is a solution to* $\mathsf{UE\text{-}PE\text{-}}\boldsymbol{X}$ *in* (13)*.*

While Lemmas 1, 2, and 3 provide sufficient conditions for a traffic flow pattern to be a κ-MSatUE, Theorem 1 of Christodoulou et al. (2011) provides a necessary condition. Although Christodoulou et al. (2011) assumed separable arc travel time functions, their proof is still valid for nonseparable travel time functions.

Lemma 4 (A necessary condition of MSatUE)**.** *Let $\boldsymbol{f}^\kappa \in \boldsymbol{F}$ be a κ-MSatUE and $\boldsymbol{v}^\kappa \in \boldsymbol{V}$ be the corresponding arc flow vector with $\boldsymbol{f}^\kappa \mapsto \boldsymbol{v}^\kappa$. Then we have*

$$\sum_{a \in \mathcal{A}} t_a(\boldsymbol{v}^\kappa)((1+\kappa)v_a - v_a^\kappa) \geq 0 \qquad \forall \boldsymbol{v} \in \boldsymbol{V}. \tag{17}$$

Christodoulou et al. (2011) derive a tight bound on the price of anarchy on approximate Nash equilibria based on Lemma 4.

Implications in Lemmas 1–4 are summarized in Figure 1. Note that this result does not mean that the notions of UE-PE and SatUE are equivalent in general. Rather, the specific modeling of $\mathsf{UE\text{-}PE\text{-}}\boldsymbol{X}$, $\mathsf{UE\text{-}PE\text{-}}\boldsymbol{F}$, and $\mathsf{UE\text{-}PE\text{-}}\boldsymbol{V}$ with the perception error interval $[\frac{1}{1+\kappa}, 1]$, as defined in (13), (15), and (16), respectively, leads to the result in Figure 1. If we use a different definition of perception error sets, such a result may not hold.

4 Bounding the Price of Satisficing

We first provide analytical bounds of $C(\boldsymbol{f}^\kappa)$ compared to $C(\boldsymbol{f}^0)$.

4.1 Lessons from the Price of Anarchy

We first observe that $\mathsf{PoSat}_\kappa(G, \boldsymbol{Q}, \boldsymbol{t}) \leq \mathsf{PoA}_\kappa(G, \boldsymbol{Q}, \boldsymbol{t})$ for any network instance $(G, \boldsymbol{Q}, \boldsymbol{t})$, since $C(\boldsymbol{f}^0) \geq C(\boldsymbol{f}^*)$. This enables us to use the results from the price of anarchy literature for bounding

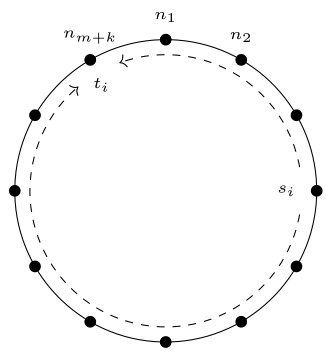

Figure 2: Circular Network of Christodoulou et al. (2011)

PoSat. Theorem 2 of Christodoulou et al. (2011) provides the price of anarchy for the general polynomial cases, which immediately leads to the following result:

Lemma 5. *Suppose $\boldsymbol{f}^\kappa$ is a κ-MSatUE flow, and $t_a(\cdot)$ is a polynomial with degree n. Define*

$$\zeta(\kappa, n) = \begin{cases} (1+\kappa)^{n+1} & \text{if } \kappa \geq (n+1)^{1/n} - 1, \\ \left(\frac{1}{1+\kappa} - \frac{n}{(n+1)^{(n+1)/n}} \right)^{-1} & \text{if } 0 \leq \kappa \leq (n+1)^{1/n} - 1. \end{cases} \tag{18}$$

Then we have

$$C(\boldsymbol{f}^*) \leq C(\boldsymbol{f}^\kappa) \leq \zeta(\kappa, n) C(\boldsymbol{f}^*) \leq \zeta(\kappa, n) C(\boldsymbol{f}^0). \tag{19}$$

That is, the PoSat is bounded above by $\zeta(\kappa, n)$.

Proof of Lemma 5. From Theorem 2 of Christodoulou et al. (2011), we have

$$C(\boldsymbol{f}^\kappa) \leq \zeta(\kappa, n) C(\boldsymbol{f}) \quad \forall \boldsymbol{f} \in \boldsymbol{F}. \tag{20}$$

Picking $\boldsymbol{f} = \boldsymbol{f}^0$ in (20), we obtain the upper bound on $C(\boldsymbol{f}^\kappa)$. Inequalities involving $C(\boldsymbol{f}^*)$ are from the fact $C(\boldsymbol{f}^*) \leq C(\boldsymbol{f})$ for all $\boldsymbol{f} \in \boldsymbol{F}$. □

With the bounds of $C(\boldsymbol{f}^\kappa)$ given in Lemma 5, it is unclear if $\zeta(\kappa, n)$ is a tight bound. Since $\zeta(\kappa, n)$ is obtained from the comparison between $C(\boldsymbol{f}^\kappa)$ and $C(\boldsymbol{f}^*)$, it is unclear if there is a case when we indeed have $C(\boldsymbol{f}^\kappa) = \zeta(\kappa, n) C(\boldsymbol{f}^0)$. We know that $\zeta(\kappa, n)$ is not tight, however, when κ is small, since $\zeta(0, n)$ is not equal to 1.

In Lemma 3 of Christodoulou et al. (2011), the existence of a network instance with $C(\boldsymbol{f}^\kappa) = (1+\kappa)^{n+1} C(\boldsymbol{f}^*)$ is shown for $\kappa \geq (n+1)^{1/n} - 1$ via a circular network example presented in Figure 2. The circular network includes $m + l$ nodes where positive integers m and l are chosen so that $\frac{m}{l} = 1 + \kappa$ or $\frac{m}{l}$ is sufficiently close to $1 + \kappa$. All nodes lie in a circle, and each node n_i is connected to nodes n_{i+1} and n_{i-1} by an *undirected* arc. The arc cost function for arc a is $t_a(v_a) = (v_a)^n$, where v_a is the total arc flow in arc a. There are $m + l$ OD pairs, $w_i = (s_i, t_i)$ for $i = 1, 2, .., m + l$, with unit demand from origin $s_i = n_i$ to destination $t_i = n_{i+m}$ (indices are taken cyclically). Note that the circular network can be easily converted to a directed network by replacing each undirected arc with two directed arcs with opposite direction. The cost associated with arc a will be $t_a(v_a, \widehat{v}_a) = (v_a + \widehat{v}_a)^n$ in this case where $\widehat{v}_a$ is the flow in the arc with opposite direction.

Clearly, for each OD pair, there are exactly two simple paths that connect s_i to t_i; namely, the clockwise path using m arcs and the counterclockwise path using l arcs. This example, however, is valid for all $\kappa \geq 0$. Note that, in this example, the system optimal flow is also at (perfectly rational) user equilibrium. If all network users choose the counterclockwise path, the (perfectly rational) user equilibrium is achieved and the flow in each arc will be equal to l, the path cost for each OD pair will be l^{n+1}, and the system total travel cost will be $(m+l)l^{n+1}$. If all network users choose the clockwise path, the flow in each arc will be equal to m, the path cost for each OD pair will be m^{n+1}. The alternative path has l arcs and the cost associated with that path will be lm^n. Since $\frac{m}{l} = (1+\kappa)$, the clockwise path will be a satisficing path. The system total travel cost will be $(m+l)m^{n+1}$. This gives $\mathsf{PoSat}_\kappa = (1+\kappa)^n$ for all $\kappa \geq 0$.

We can also observe that the $\mathsf{UE\text{-}PE\text{-}}\boldsymbol{X}$ model can capture the satisficing behavior of network users in the circular network adequately. If we set the value of $\boldsymbol{\lambda}$ as follow as (indices are taken cyclically):

$$\lambda_a^{w_i} = \begin{cases} \frac{1}{1+\kappa} & \text{for } a \in \{(n_j, n_{j+1}) : j = i, i+1, ..., i+m-1\} \\ 1 & \text{for } a \in \{(n_j, n_{j-1}) : j = i, i-1, ..., i-l+1\} \end{cases}$$

Under the above $\boldsymbol{\lambda}$, if all network user choose the clockwise path, the flow in each arc will be equal to m, the path cost for each OD pair will be $\frac{1}{1+k} m^{n+1} = lm^n$, which is equal to the cost of the alternative path, and thus the clockwise path is a solution to $\mathsf{UE\text{-}PE\text{-}}\boldsymbol{X}$ and $\mathsf{PoSat}_\kappa = (1+\kappa)^n$. In Section 5, we will compute the PoSat numerically for these examples to confirm that $\mathsf{UE\text{-}PE\text{-}}\boldsymbol{X}$ is a useful model to find PoSat_κ.

By Lemma 5, when travel time functions are polynomials of degree n, the PoSat is bounded as follows:

$$\mathsf{PoSat}_\kappa(G, \boldsymbol{Q}, \boldsymbol{t}) \leq \begin{cases} (1+\kappa)^{n+1} & \text{if } \kappa \geq (n+1)^{1/n} - 1, \\ \left(\frac{1}{1+\kappa} - \frac{n}{(n+1)^{(n+1)/n}} \right)^{-1} & \text{if } 0 \leq \kappa \leq (n+1)^{1/n} - 1. \end{cases} \tag{21}$$

for all $(G, \boldsymbol{Q}, \boldsymbol{t}) \in \Omega(n)$ and by the circular network example in Figure 2, we know that there indeed exists a network instance $(G, \boldsymbol{Q}, \boldsymbol{t}) \in \Omega(n)$ such that $\mathsf{PoSat}_\kappa(G, \boldsymbol{Q}, \boldsymbol{t}) = (1+\kappa)^{n+1}$ for all $\kappa \geq 0$. Therefore when $\kappa \geq (n+1)^{1/n} - 1$, the bound in (21) is tight. Figure 5a shows the bounds in (21) for the linear travel time function case. For smaller κ values, the worst-case PoSat falls in the shaded interval, while for larger κ values, it is exactly $(1+\kappa)^2$. Figure 5b is for $n = 4$. When κ is zero, we have $\boldsymbol{f}^\kappa = \boldsymbol{f}^0$; hence, we must have the PoSat approach to 1. With this observation, we naturally ask a question: Does $(1+\kappa)^{n+1}$ provide a tight bound on PoSat_κ for all $\kappa \geq 0$? We present partial answers to this question in the following sections.

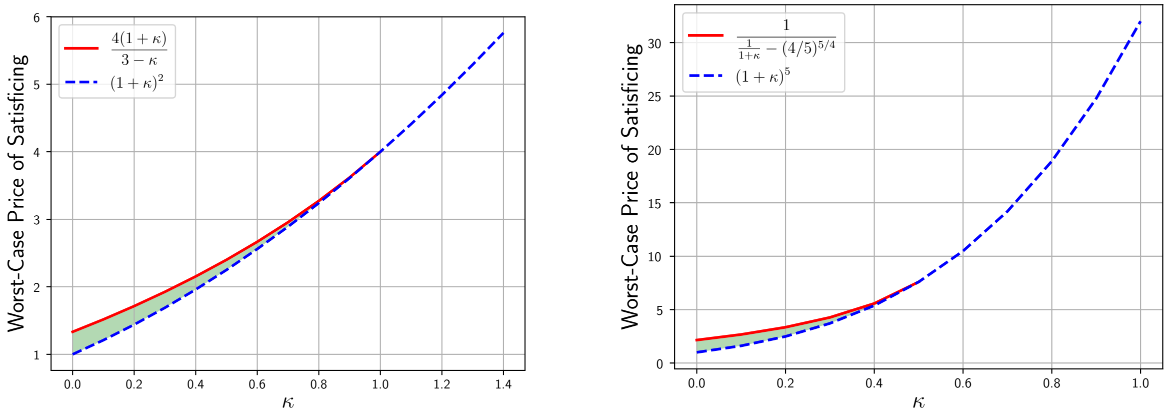

(a) $n = 1$ (b) $n = 4$

Figure 3: The worst-case price of satisficing for $n = 1$ and $n = 4$. Note that when $n = 1$, the right-hand-side of (21) becomes $\frac{4(1+\kappa)}{3-\kappa}$. For $n = 1$, when $\kappa \geq 1$, we know for sure that the worst-case price of satisficing is exactly the dotted line. When $\kappa \leq 1$, the worst case falls in the shaded interval between the solid line and dotted line. When $n = 4$, it is similar.

4.2 Increased Travel Demands and Travel Time Functions

We first define new sets of flow vectors. When the travel demand Q_w for each $w \in \mathcal{W}$ is multiplied by the factor $1 + \kappa$, we define

$$\begin{aligned}
\boldsymbol{F}_{1+\kappa} &= \left\{ \boldsymbol{f} : \sum_{p \in \mathcal{P}_w} f_p = (1+\kappa) Q_w \quad \forall w \in \mathcal{W}, \qquad f_p \geq 0 \quad \forall p \in \mathcal{P} \right\}, \\
\boldsymbol{V}_{1+\kappa} &= \left\{ \boldsymbol{v} : v_a = \sum_{p \in \mathcal{P}} \delta_a^p f_p \quad \forall a \in \mathcal{A}, \qquad \boldsymbol{f} \in \boldsymbol{F}_{1+\kappa} \right\}, \\
\boldsymbol{X}_{1+\kappa} &= \left\{ \boldsymbol{x} : x_a^w = \sum_{p \in \mathcal{P}_w} \delta_a^p f_p \quad \forall a \in \mathcal{A}, w \in \mathcal{W} \qquad \boldsymbol{f} \in \boldsymbol{F}_{1+\kappa} \right\}.
\end{aligned}$$

The above three sets can equivalently be written as follows:

$$\begin{aligned}
\boldsymbol{F}_{1+\kappa} &= \{(1+\kappa)\boldsymbol{f} : \boldsymbol{f} \in \boldsymbol{F}\}, \\
\boldsymbol{V}_{1+\kappa} &= \{(1+\kappa)\boldsymbol{v} : \boldsymbol{v} \in \boldsymbol{V}\}, \\
\boldsymbol{X}_{1+\kappa} &= \{(1+\kappa)\boldsymbol{x} : \boldsymbol{x} \in \boldsymbol{X}\}.
\end{aligned}$$

We will use 'hat' for flow vectors in these sets, for example, $\widehat{\boldsymbol{f}}^\kappa \in \boldsymbol{F}_{1+\kappa}$, while without hat in the original sets as in $\boldsymbol{f}^\kappa \in \boldsymbol{F}$.

We consider cases when the travel time functions $t_a(\cdot)$ are polynomials of order n, in particular, the following form of *asymmetric* arc travel time function for each $a \in \mathcal{A}$:

$$t_a(\boldsymbol{v}) = \sum_{m=0}^{n} b_{am} \left(\sum_{e \in \mathcal{A}} d_{aem} v_e \right)^m = \sum_{m=0}^{n} b_{am} \left(\boldsymbol{d}_{am}^\top \boldsymbol{v} \right)^m \tag{22}$$

for some constants b_{am} for $m = 0, 1, ..., n$ and d_{aem} for $e \in \mathcal{A}$ and $m = 0, 1, ..., n$. Note that we use the vector form $\boldsymbol{d}_{am} = (d_{aem} : e \in \mathcal{A})$. The travel time function (22) is a general form of the travel time functions considered in the traffic equilibrium literature (Meng et al., 2014; Panicucci et al., 2007). If $\boldsymbol{d}_{am}$ is a unit vector such that d_{aem} is 1 if $a = e$ and 0 otherwise, we have a separable polynomial arc travel time function that has been used in the literature popularly (Christodoulou et al., 2011; Roughgarden and Tardos, 2002):

$$t_a(v_a) = \sum_{m=0}^{n} b_{am}(v_a)^m = b_{a0} + b_{a1}v_a + b_{a2}(v_a)^2 + \cdots + b_{an}(v_a)^n. \tag{23}$$

Lemma 6. *With the polynomial travel time function* (22)*, for any* $\boldsymbol{f} \in \boldsymbol{F}$*, we have*

$$C((1+\kappa)\boldsymbol{f}) \leq (1+\kappa)^{n+1} C(\boldsymbol{f}) \tag{24}$$

for all $\kappa \geq 0$ *and* $n \geq 0$*.*

Proof of Lemma 6. By simple comparison, we can show

$$\begin{aligned} C((1+\kappa)\boldsymbol{f}) = Z((1+\kappa)\boldsymbol{v}) &= \sum_{a \in \mathcal{A}} \left(\sum_{m=0}^{n} b_{am} \left((1+\kappa) \boldsymbol{d}_{am}^\top \boldsymbol{v} \right)^m \right) (1+\kappa) v_a \\ &\leq (1+\kappa)^{n+1} \left(\sum_{m=0}^{n} b_{am} \left(\boldsymbol{d}_{am}^\top \boldsymbol{v} \right)^m \right) v_a \\ &= (1+\kappa)^{n+1} Z(\boldsymbol{v}) \\ &= (1+\kappa)^{n+1} C(\boldsymbol{f}) \end{aligned}$$

where $\boldsymbol{v}$ is the arc flow vector from $\boldsymbol{f} \mapsto \boldsymbol{v}$. □

4.3 Cases with Separable, Monomial Arc Travel Time Functions

As a simple case, we consider separable, monomial functions of degree n for arc travel time of the following form:

$$t_a(v_a) = b_a(v_a)^n \tag{25}$$

with a positive scalar b_a for each $a \in \mathcal{A}$ and nonnegative constant n.

It is well known (Beckmann et al., 1956) that $\boldsymbol{v}^0 \in \boldsymbol{F}$ is a user equilibrium flow, if and only if it minimizes the following potential function

$$\Phi(\boldsymbol{v}) = \sum_{a\in\mathcal{A}} \int_0^{v_a} t_a(u)\,\mathrm{d}u = \sum_{a\in\mathcal{A}} \frac{b_a}{n+1}(v_a)^{n+1}$$

when the arc travel time functions are separable, so that the integral is well defined. Similarly, $\boldsymbol{v}^\kappa \in \boldsymbol{V}$ is a κ-MSatUE flow, if it is a solution to $\mathsf{UE\text{-}PE}\text{-}\boldsymbol{V}$, or equivalently, if it minimizes the following potential function (Christodoulou et al., 2011)

$$\Psi(\boldsymbol{v};\boldsymbol{\lambda}) = \sum_{a\in\mathcal{A}} \int_0^{v_a} \lambda_a t_a(u)\,\mathrm{d}u = \sum_{a\in\mathcal{A}} \frac{\lambda_a b_a}{n+1}(v_a)^{n+1}$$

for some $\lambda_a \in [\frac{1}{1+\kappa}, 1]$ for each $a \in \mathcal{A}$.

When travel time functions are separable, we can show the following result (Englert et al., 2010; Takalloo and Kwon, 2018):

Lemma 7. *When the arc travel time functions are in the form of* (23)*, let $\boldsymbol{f}^0 \in \boldsymbol{F}$ and $\widehat{\boldsymbol{f}}^0 \in \boldsymbol{F}_{1+\kappa}$ be the PRUE flows with the corresponding travel demands. We can show*

$$C(\widehat{\boldsymbol{f}}^0) \leq (1+\kappa)^{n+1} C(\boldsymbol{f}^0) \tag{26}$$

for all $\kappa \geq 0$ and $n \geq 0$.

Although Englert et al. (2010) consider cases with a single OD pair only with interest in the changes in the path travel time, the same technique can be used to prove Lemma 7 for cases with multiple OD pairs. For completeness, we include the proof to Lemma 7 in the appendix.

Using Lemma 7, we show that a solution to $\mathsf{UE\text{-}PE}\text{-}\boldsymbol{V}$ is an MSatUE flow.

Theorem 1. *When the arc travel time functions are of the form* (25)*, let $\bar{\boldsymbol{v}} \in \boldsymbol{V}$ be a solution to $\mathsf{UE\text{-}PE}\text{-}\boldsymbol{V}$ and $\bar{\boldsymbol{f}} \in \boldsymbol{F}$ is the any corresponding path flow with $\bar{\boldsymbol{v}} \xmapsto{\text{any}} \bar{\boldsymbol{f}}$. We let $\widehat{\boldsymbol{f}}^0 \in \boldsymbol{F}_{1+\kappa}$ be the PRUE flows. Then we have $C(\boldsymbol{f}^\kappa) \leq C(\widehat{\boldsymbol{f}}^0)$, and consequently $C(\boldsymbol{f}^\kappa) \leq (1+\kappa)^{n+1} C(\boldsymbol{f}^0)$ for all $\kappa \geq 0$.*

Proof of Theorem 1. Since $\widehat{\boldsymbol{v}}^0 \in \boldsymbol{F}_{1+\kappa}$ is an user equilibrium flow that minimizes $\Phi(\cdot)$, we have

$$\Phi(\widehat{\boldsymbol{v}}^0) \leq \Phi\big((1+\kappa)\bar{\boldsymbol{v}}\big),$$

which implies

$$\sum_{a\in\mathcal{A}} \frac{b_a(\widehat{v}_a^0)^{n+1}}{n+1} \leq \sum_{a\in\mathcal{A}} \frac{b_a\big((1+\kappa)\bar{v}_a\big)^{n+1}}{n+1} = (1+\kappa)^{n+1} \sum_{a\in\mathcal{A}} \frac{b_a(\bar{v}_a)^{n+1}}{n+1}. \tag{27}$$

Since $\bar{\boldsymbol{v}} \in \boldsymbol{V}$ is a solution to $\mathsf{UE\text{-}PE}\text{-}\boldsymbol{V}$, we have

$$\Psi(\bar{\boldsymbol{v}};\boldsymbol{\lambda}) \leq \Psi\Big(\frac{\widehat{\boldsymbol{v}}^0}{1+\kappa};\boldsymbol{\lambda}\Big),$$

for some $\boldsymbol{\lambda}$. Therefore, we have

$$\sum_{a\in\mathcal{A}} \frac{\lambda_a b_a(\bar{v}_a)^{n+1}}{n+1} \le \sum_{a\in\mathcal{A}} \frac{\lambda_a b_a(v_a^0)^{n+1}}{(n+1)(1+\kappa)^{n+1}} = \frac{1}{(1+\kappa)^{n+1}} \sum_{a\in\mathcal{A}} \frac{\lambda_a b_a(\widehat{v}_a^0)^{n+1}}{n+1}.$$

Since $\lambda_a \in [\frac{1}{1+\kappa}, 1]$, we obtain

$$\frac{1}{1+\kappa} \sum_{a\in\mathcal{A}} \frac{b_a(\bar{v}_a)^{n+1}}{n+1} \le \frac{1}{(1+\kappa)^{n+1}} \sum_{a\in\mathcal{A}} \frac{b_a(\widehat{v}_a^0)^{n+1}}{n+1}$$

which implies

$$(1+\kappa)^n \sum_{a\in\mathcal{A}} \frac{b_a(\bar{v}_a)^{n+1}}{n+1} \le \sum_{a\in\mathcal{A}} \frac{b_a(\widehat{v}_a^0)^{n+1}}{n+1} \tag{28}$$

Let us assume that $C(\bar{\boldsymbol{f}}) > C(\widehat{\boldsymbol{f}}^0)$, which is equivalent to

$$\sum_{a\in\mathcal{A}} b_a(\widehat{v}_a^0)^{n+1} < \sum_{a\in\mathcal{A}} b_a(\bar{v}_a)^{n+1} \tag{29}$$

From $A \times (27) + B \times (28) + C \times (29)$ for any positive constants A, B and C, we obtain

$$\theta_1 \sum_{a\in\mathcal{A}} \frac{b_a(\widehat{v}_a^0)^{n+1}}{n+1} < \theta_2 \sum_{a\in\mathcal{A}} \frac{b_a(\bar{v}_a)^{n+1}}{n+1} \tag{30}$$

where

$$\begin{aligned} \theta_1 &= A - B + C(n+1) \\ \theta_2 &= A(1+\kappa)^{n+1} - B(1+\kappa)^n + C(n+1). \end{aligned}$$

In particular, consider A, B and C as follows:

$$\begin{aligned} A &= (n+1)\big((1+\kappa)^n - 1\big) \\ B &= (n+1)\big((1+\kappa)^n - 1\big) + (n+1)\kappa(1+\kappa)^{n+1} \\ C &= \kappa(1+\kappa)^{n+1} \end{aligned}$$

We observe that A, B and C are all positive and $\theta_1 = 0$. We also see that

$$\theta_2 = -(n+1)\kappa^2(1+\kappa)^n\big((1+\kappa)^{n+1} - 1\big) \le 0$$

for all $\kappa \ge 0$ and $n \ge 0$, which leads to a contradiction. Therefore, we have

$$C(\bar{\boldsymbol{f}}) \le C(\widehat{\boldsymbol{f}}^0) \le (1+\kappa)^{n+1} C(\boldsymbol{f}^0),$$

where the last inequality is from Lemma 7. This completes the proof. □

Note that the bound obtained in Theorem 1 relies on the sufficient condition, not a necessary condition. Therefore, the result is not applicable to all MSatUE flows, although it provides a useful bound in the framework of UE-PE models.

4.4 Cases with Separable Arc Travel Time Functions

We consider general polynomial, separable arc travel functions in the form of (23).

Theorem 2. *Suppose that the arc travel time functions are in the form of* (23). *Let* $\boldsymbol{f}^\kappa \in \boldsymbol{F}$ *be any* κ*-MSatUE and* $\widehat{\boldsymbol{f}}^0 \in \boldsymbol{F}_{1+\kappa}$ *be the PRUE flow. Suppose that* $\kappa \geq 0$ *is sufficiently small, in particular, so that*

$$\sum_{p\in\mathcal{P}} [c_p(\widehat{\boldsymbol{f}}^0) - c_p(\boldsymbol{f}^\kappa)](\widehat{f}_p^0 - f_p^\kappa) \geq \kappa \sum_{p\in\mathcal{P}} c_p(\boldsymbol{f}^\kappa) \left| \widehat{f}_p^0 - f_p^\kappa \right|. \tag{31}$$

Then we have $C(\boldsymbol{f}^\kappa) \leq C(\widehat{\boldsymbol{f}}^0)$. *Consequently* $C(\boldsymbol{f}^\kappa) \leq (1+\kappa)^{n+1} C(\boldsymbol{f}^0)$, *and*

$$\sup_{(G,\boldsymbol{Q},\boldsymbol{t})\in\Omega(n)} \mathsf{PoSat}_\kappa(G,\boldsymbol{Q},\boldsymbol{t}) = (1+\kappa)^{n+1}.$$

Proof of Theorem 2. By slightly modifying the proof of Theorem 3, we can show $C(\boldsymbol{f}^\kappa) \leq C(\widehat{\boldsymbol{f}}^0)$. By Lemmas 6 and 7, we complete the proof. □

Theorem 2 depends on condition (31) and a similar condition appears in general asymmetric cases as in Theorem 3. We discuss this condition in Section 4.6.

4.5 General Cases with Asymmetric Arc Travel Time Functions

We consider asymmetric arc travel time functions (22), in which case Lemma 7 is not applicable. We first observe that the multiple of a PRUE flow, $(1+\kappa)\boldsymbol{f}^0$, provides a satisficing solution to the traffic equilibrium problem with the increased travel demand.

Lemma 8. *Suppose* $t_a(\cdot)$ *are polynomials of order* n *as defined* (22). *If* $\boldsymbol{f}^0 \in \boldsymbol{F}$ *is a PRUE flow, then* $(1+\kappa)\boldsymbol{f}^0$ *is a* σ*-MSatUE flow with* $\sigma = (1+\kappa)^n - 1$ *in* $\boldsymbol{F}_{1+\kappa}$. *When* $n = 1$, *we have* $\sigma = \kappa$.

Proof. Let $\bar{\boldsymbol{f}} = (1+\kappa)\boldsymbol{f}^0$, and $\bar{\boldsymbol{v}} = (1+\kappa)\boldsymbol{v}^0$ for the corresponding arc flow vectors. If the condition

$$\sum_{a\in\mathcal{A}} \left(\sum_{m=0}^{n} \lambda_{am} b_{am} \left(\boldsymbol{d}_{am}^\top \bar{\boldsymbol{v}} \right)^m \right) (v'_a - \bar{v}_a) \geq 0 \qquad \forall \boldsymbol{v}' \in \boldsymbol{V}_{1+\kappa} \tag{32}$$

holds for some constants $\lambda_{am} \in [\frac{1}{1+\sigma}, 1]$ for $m = 0, 1, ..., n$ and $a \in \mathcal{A}$, then we can find $\lambda_a \in [\frac{1}{1+\sigma}, 1]$ such that

$$\lambda_a \sum_{m=0}^{n} b_{am} \left(\boldsymbol{d}_{am}^\top \bar{\boldsymbol{v}} \right)^m = \sum_{m=0}^{n} \lambda_{am} b_{am} \left(\boldsymbol{d}_{am}^\top \bar{\boldsymbol{v}} \right)^m$$

for all $a \in \mathcal{A}$; consequently, by Lemmas 1 and 3, $\bar{\boldsymbol{f}}$ is a σ-MSatUE flow in $\boldsymbol{F}_{1+\kappa}$.

Since $\boldsymbol{v}^0$ is PRUE for $\boldsymbol{V}$, we know that

$$\sum_{a\in\mathcal{A}}\left(\sum_{m=0}^{n} b_{am}\left(\boldsymbol{d}_{am}^{\top}\boldsymbol{v}^0\right)^m\right)(v_a - v_a^0) \geq 0 \qquad \forall \boldsymbol{v} \in \boldsymbol{V}.$$

Therefore

$$\sum_{a\in\mathcal{A}}\left(\sum_{m=0}^{n} \frac{1}{(1+\kappa)^m} b_{am}\left((1+\kappa)\boldsymbol{d}_{am}^{\top}\boldsymbol{v}^0\right)^m\right)((1+\kappa)v_a - (1+\kappa)v_a^0) \geq 0 \qquad \forall \boldsymbol{v} \in \boldsymbol{V}.$$

Letting for all $a \in \mathcal{A}$

$$\begin{aligned} \lambda_{am} &= \frac{1}{(1+\kappa)^m}, \qquad m = 0, 1, ..., n \\ \bar{v}_a &= (1+\kappa)v_a^0, \\ v'_a &= (1+\kappa)v_a, \end{aligned}$$

we observe that $\lambda_{am} \in [\frac{1}{1+\sigma}, 1]$ and we obtain (32); hence proof. □

By introducing an additional condition, we compare MSatUE flows with the proportional travel demand increase, and obtain the worst-case bound of PoSat.

Theorem 3. *Let $\boldsymbol{f}^\kappa \in \boldsymbol{F}$ be any κ-MSatUE and $\widehat{\boldsymbol{f}}^\sigma \in \boldsymbol{F}_{1+\kappa}$ be any σ-MSatUE flows with the corresponding travel demands, when $\sigma = (1+\kappa)^n - 1$. Suppose that $\kappa \geq 0$ is sufficiently small, in particular, so that*

$$\sum_{p\in\mathcal{P}}[c_p(\widehat{\boldsymbol{f}}^\sigma) - c_p(\boldsymbol{f}^\kappa)](\widehat{f}_p^\sigma - f_p^\kappa) \geq \sigma \sum_{p\in\mathcal{P}} \max\{c_p(\widehat{\boldsymbol{f}}^\sigma), c_p(\boldsymbol{f}^\kappa)\}\left|\widehat{f}_p^\sigma - f_p^\kappa\right|. \tag{33}$$

Then we have $C(\boldsymbol{f}^\kappa) \leq C(\widehat{\boldsymbol{f}}^\sigma)$. Consequently $C(\boldsymbol{f}^\kappa) \leq (1+\kappa)^{n+1}C(\boldsymbol{f}^0)$, and

$$\sup_{(G,\boldsymbol{Q},\boldsymbol{t})\in\Omega(n)} \mathsf{PoSat}_\kappa(G,\boldsymbol{Q},\boldsymbol{t}) = (1+\kappa)^{n+1}.$$

Proof of Theorem 3. We decompose $\mathcal{P}_w$ for each OD pair w into the following four subsets:

$$\begin{aligned} \mathcal{P}_w^1 &= \{p \in \mathcal{P}_w : \widehat{f}_p^\sigma > 0,\ f_p^\kappa > 0,\ \widehat{f}_p^\sigma - f_p^\kappa \geq 0\}, \\ \mathcal{P}_w^2 &= \{p \in \mathcal{P}_w : \widehat{f}_p^\sigma > 0,\ f_p^\kappa > 0,\ \widehat{f}_p^\sigma - f_p^\kappa < 0\}, \\ \mathcal{P}_w^3 &= \{p \in \mathcal{P}_w : \widehat{f}_p^\sigma > 0,\ f_p^\kappa = 0\}, \\ \mathcal{P}_w^4 &= \{p \in \mathcal{P}_w : \widehat{f}_p^\sigma = 0,\ f_p^\kappa > 0\}. \end{aligned}$$

We ignore cases with $\widehat{f}_p^\sigma = 0$ and $f_p^\kappa = 0$. Note that $\widehat{f}_p^\sigma - f_p^\kappa > 0$ for $p \in \mathcal{P}_w^3$ and $\widehat{f}_p^\sigma - f_p^\kappa < 0$ for

$p \in \mathcal{P}_w^4$. From the definition of MSatUE flows, we have

$$\widehat{f}_p^\sigma > 0 \implies c_p(\widehat{\boldsymbol{f}}^\sigma) \le (1+\sigma)\mu_w(\widehat{\boldsymbol{f}}^\sigma),$$
$$f_p^\kappa > 0 \implies c_p(\boldsymbol{f}^\kappa) \le (1+\kappa)\mu_w(\boldsymbol{f}^\kappa),$$

for all $p \in \mathcal{P}_w, w \in \mathcal{W}$. In addition, $\mu_w(\widehat{\boldsymbol{f}}^\sigma) \le c_p(\widehat{\boldsymbol{f}}^\sigma)$ and $\mu_w(\boldsymbol{f}^\kappa) \le c_p(\boldsymbol{f}^\kappa)$ for all $p \in \mathcal{P}$ by definition. Therefore, we have

$$\begin{aligned}
&\sum_{p\in\mathcal{P}}[c_p(\widehat{\boldsymbol{f}}^\sigma) - c_p(\boldsymbol{f}^\kappa)](\widehat{f}_p^\sigma - f_p^\kappa) \\
&\le \sum_{w\in\mathcal{W}} \Bigg\{ \sum_{p\in\mathcal{P}_w^1} \Big[(1+\sigma)\mu_w(\widehat{\boldsymbol{f}}^\sigma) - \mu_w(\boldsymbol{f}^\kappa)\Big](\widehat{f}_p^\sigma - f_p^\kappa) + \sum_{p\in\mathcal{P}_w^2} \Big[\mu_w(\widehat{\boldsymbol{f}}^\sigma) - (1+\kappa)\mu_w(\boldsymbol{f}^\kappa)\Big](\widehat{f}_p^\sigma - f_p^\kappa) \\
&\qquad + \sum_{p\in\mathcal{P}_w^3} \Big[(1+\sigma)\mu_w(\widehat{\boldsymbol{f}}^\sigma) - \mu_w(\boldsymbol{f}^\kappa)\Big](\widehat{f}_p^\sigma - f_p^\kappa) + \sum_{p\in\mathcal{P}_w^4} \Big[\mu_w(\widehat{\boldsymbol{f}}^\sigma) - (1+\kappa)\mu_w(\boldsymbol{f}^\kappa)\Big](\widehat{f}_p^\sigma - f_p^\kappa) \Bigg\} \\
&= \sum_{w\in\mathcal{W}} \Bigg\{ \sum_{p\in\mathcal{P}_w} \Big[\mu_w(\widehat{\boldsymbol{f}}^\sigma) - \mu_w(\boldsymbol{f}^\kappa)\Big](\widehat{f}_p^\sigma - f_p^\kappa) + \sigma \sum_{p\in\mathcal{P}_w^1\cup\mathcal{P}_w^3} \mu_w(\widehat{\boldsymbol{f}}^\sigma)(\widehat{f}_p^\sigma - f_p^\kappa) \\
&\qquad - \kappa \sum_{p\in\mathcal{P}_w^2\cup\mathcal{P}_w^4} \mu_w(\boldsymbol{f}^\kappa)(\widehat{f}_p^\sigma - f_p^\kappa) \Bigg\} \\
&\le \sum_{w\in\mathcal{W}} \Bigg\{ \sum_{p\in\mathcal{P}_w} \Big[\mu_w(\widehat{\boldsymbol{f}}^\sigma) - \mu_w(\boldsymbol{f}^\kappa)\Big](\widehat{f}_p^\sigma - f_p^\kappa) + \sigma \sum_{p\in\mathcal{P}_w} \max\{\mu_w(\widehat{\boldsymbol{f}}^\sigma), \mu_w(\boldsymbol{f}^\kappa)\}\Big|\widehat{f}_p^\sigma - f_p^\kappa\Big| \Bigg\} \\
&\le \sum_{w\in\mathcal{W}} \sum_{p\in\mathcal{P}_w} \Big[\mu_w(\widehat{\boldsymbol{f}}^\sigma) - \mu_w(\boldsymbol{f}^\kappa)\Big](\widehat{f}_p^\sigma - f_p^\kappa) + \sigma \sum_{p\in\mathcal{P}} \max\{c_p(\widehat{\boldsymbol{f}}^\sigma), c_p(\boldsymbol{f}^\kappa)\}\Big|\widehat{f}_p^\sigma - f_p^\kappa\Big|.
\end{aligned}$$

From (33), we obtain

$$\begin{aligned}
0 &\le \sum_{w\in\mathcal{W}} \sum_{p\in\mathcal{P}} \Big[\mu_w(\widehat{\boldsymbol{f}}^\sigma) - \mu_w(\boldsymbol{f}^\kappa)\Big](\widehat{f}_p^\sigma - f_p^\kappa) \\
&= \sum_{w\in\mathcal{W}} \Big[\mu_w(\widehat{\boldsymbol{f}}^\sigma) - \mu_w(\boldsymbol{f}^\kappa)\Big]\Bigg(\sum_{p\in\mathcal{P}} \widehat{f}_p^\sigma - \sum_{p\in\mathcal{P}} f_p^\kappa\Bigg) \\
&= \sum_{w\in\mathcal{W}} \Big[\mu_w(\widehat{\boldsymbol{f}}^\sigma) - \mu_w(\boldsymbol{f}^\kappa)\Big](\widehat{Q}_w - Q_w) \\
&= \kappa \sum_{w\in\mathcal{W}} \mu_w(\widehat{\boldsymbol{f}}^\sigma) Q_w - \kappa \sum_{w\in\mathcal{W}} \mu_w(\boldsymbol{f}^\kappa) Q_w \\
&= \frac{\kappa}{1+\kappa} \sum_{w\in\mathcal{W}} \mu_w(\widehat{\boldsymbol{f}}^\sigma) \widehat{Q}_w - \kappa \sum_{w\in\mathcal{W}} \mu_w(\boldsymbol{f}^\kappa) Q_w \\
&\le \frac{\kappa}{1+\kappa} \sum_{w\in\mathcal{W}} \sum_{p\in\mathcal{P}_w} c_p(\widehat{\boldsymbol{f}}^\sigma) \widehat{f}_p^\sigma - \frac{\kappa}{1+\kappa} \sum_{w\in\mathcal{W}} \sum_{p\in\mathcal{P}_w} c_p(\boldsymbol{f}^\kappa) f_p^\kappa \\
&= \frac{\kappa}{1+\kappa} C(\widehat{\boldsymbol{f}}^\sigma) - \frac{\kappa}{1+\kappa} C(\boldsymbol{f}^\kappa).
\end{aligned}$$

Lemmas 6 and 8 complete the proof. □

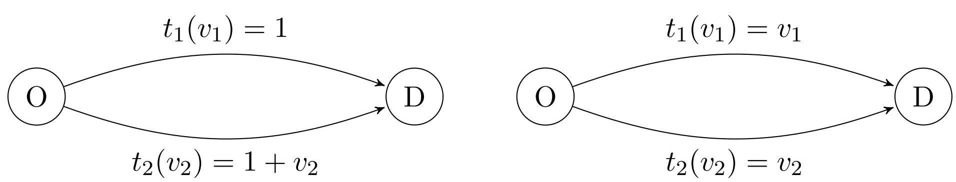

(a) Example 1 (b) Example 2

Figure 4: Examples where the travel demand is Q from node O to node D.

Note that condition (33) is stronger than condition (31) for separable travel time functions. This is natural, since we consider more general classes of travel time functions.

4.6 Illustrative Examples

For the illustration purpose, we consider two examples in Figure 4 with linear travel time functions, where $n = 1$. In Example 1, the travel time function in the first arc is not increasing. We can verify that

$$\max C(\boldsymbol{f}^\kappa) = \begin{cases} Q + \kappa^2 & \text{if } \kappa \le Q, \qquad \text{with } \boldsymbol{f}^\kappa = (Q - \kappa, \kappa) \\ (1+Q)Q & \text{if } \kappa \ge Q, \qquad \text{with } \boldsymbol{f}^\kappa = (0, Q) \end{cases}$$

among all κ-MSatUE flows in $\boldsymbol{F}$ and

$$C(\widehat{\boldsymbol{f}}^0) = (1+\kappa)Q \qquad \text{with } \widehat{\boldsymbol{f}}^0 = (1+\kappa)\boldsymbol{f}^0 = ((1+\kappa)Q, 0).$$

among all κ-MSatUE flows in $\boldsymbol{F}_{1+\kappa}$. Comparing the two quantities, we observe $C(\boldsymbol{f}^\kappa) \le C(\widehat{\boldsymbol{f}}^0)$ in both cases. To prove Theorem 3, condition (31) needs to hold only for these two flow vectors. Regardless of the value of κ, however, it is impossible to satisfy condition (31), although the worst-case PoSat bound $(1+\kappa)^{n+1}$ still holds for all $\kappa \ge 0$. The price of satisficing is $1 + \frac{\kappa^2}{Q}$ if $\kappa < Q$ and $1 + Q$ if $\kappa \ge Q$ in this example, both of which are less than $(1+\kappa)^2$.

On the other hand, in Example 2, we have strictly monotone travel time functions in both arcs. Similarly, we consider

$$\max C(\boldsymbol{v}^\kappa) = \frac{2 + 2\kappa + \kappa^2}{(2+\kappa)^2} Q \qquad \text{with } \boldsymbol{f}^\kappa = \left(\frac{Q}{2+\kappa}, \frac{(1+\kappa)Q}{2+\kappa} \right)$$

$$C(\widehat{\boldsymbol{v}}^0) = \frac{(1+\kappa)^2}{2} Q \qquad \text{with } \widehat{\boldsymbol{f}}^0 = (1+\kappa)\boldsymbol{f}^0 = \left(\frac{(1+\kappa)Q}{2}, \frac{(1+\kappa)Q}{2} \right)$$

and can verify that $C(\boldsymbol{f}^\kappa) \le C(\widehat{\boldsymbol{f}}^0)$ for all $\kappa \ge 0$. In Example 2, we note that (33) holds for $\kappa \le 0.206$. In this example, we observe that the price of satisficing is $\frac{2(2+2\kappa+\kappa^2)}{(2+\kappa)^2}$, which is no greater than $(1+\kappa)^2$ for all $\kappa \ge 0$.

4.7 Other Approaches

When there is a single origin and multiple destinations, i.e., a single common origin node, in the network, Kleer and Schäfer (2016) introduces the notion of the *deviation ratio* that compares the system performances of the user equilibrium and the equilibrium with *deviated* travel time functions $\widetilde{t}_a(\cdot)$. The notion of deviation may also be interpreted as perception in our definition. In a special case, the deviation ratio is reduced to the price of risk aversion (Nikolova and Stier-Moses, 2015) that compares the performances of equilibria among risk-averse and risk-neutral network users.

Kleer and Schäfer (2016) define the (separable) deviated travel time functions with the following bounds:

$$t_a(v_a) + \alpha t_a(v_a) \leq \widetilde{t}_a(v_a) \leq t_a(v_a) + \beta t_a(v_a) \tag{34}$$

where $-1 \leq \alpha \leq 0 \leq \beta$. The consideration of this deviated travel time function generalizes our UE-PE model where $\alpha = -\frac{\kappa}{1+\kappa}$ and $\beta = 0$. Kleer and Schäfer (2016) show that the worst-case deviation ratio with (34) is bounded by

$$1 + \frac{\beta - \alpha}{1 + \alpha} \left\lceil \frac{|\mathcal{N}| - 1}{2} \right\rceil Q.$$

Therefore, we obtain the following theorem:

Theorem 4 (Kleer and Schäfer, 2016)**.** *Consider a directed graph with a single common origin node with the total travel demand Q and let $|\mathcal{N}|$ be the number of nodes. Then we have*

$$\frac{Z(\boldsymbol{v}^\kappa)}{Z(\boldsymbol{v}^0)} \leq 1 + \kappa \left\lceil \frac{|\mathcal{N}| - 1}{2} \right\rceil Q \tag{35}$$

where $\boldsymbol{v}^\kappa$ is a solution to $\mathsf{UE\text{-}PE\text{-}}\boldsymbol{V}$ *in* (16).

Note that Theorem 4 only covers a subset of the entire MSatUE flows, as it is limited to the solutions $\mathsf{UE\text{-}PE\text{-}}\boldsymbol{V}$ in (16) and is applicable to cases with a *single* common origin. When Theorem 4 is applied in the examples in Figure 4, the bound (35) becomes $1 + \kappa Q$.

5 Numerical Bounds

To quantify PoSat in typical traffic networks and compare it with the analytical bound obtained in Theorem 3, we define the worst-case problem for the total system travel time under MSatUE as follows:

$$\begin{aligned} \max_{\boldsymbol{v}^\kappa} \quad & Z(\boldsymbol{v}^\kappa) = \sum_{a \in \mathcal{A}} z_a(v_a^\kappa) = \sum_{a \in \mathcal{A}} t_a(\boldsymbol{v}^\kappa) v_a^\kappa \\ \text{subject to} \quad & \boldsymbol{v}^\kappa \text{ is an } \underline{\text{MSatUE}} \text{ flow with } \kappa \end{aligned} \tag{36}$$

To quantify the benefit of satisficing, instead of maximizing, we can minimize the objective function (36). Since MSatUE involves path-based definition and formulation, (36) is numerically more challenging to solve. Instead, we replace MSatUE by $\mathsf{UE\text{-}PE\text{-}}\boldsymbol{X}$. We know that the $\mathsf{UE\text{-}PE\text{-}}\boldsymbol{X}$. models provide a subset of MSatUE traffic flow patterns as seen in Lemmma 1; hence by using $\mathsf{UE\text{-}PE\text{-}}\boldsymbol{X}$ models, we will obtain suboptimal solutions to (36).

Using $\mathsf{UE\text{-}PE\text{-}}\boldsymbol{X}$ in (12), we formulate the worst-case problem as follows:

$$
\begin{aligned}
\max_{\bar{\boldsymbol{v}},\bar{\boldsymbol{x}},\boldsymbol{\varepsilon}} \quad & Z(\bar{\boldsymbol{v}}) = \sum_{a\in\mathcal{A}} z_a(\bar{\boldsymbol{v}}) = \sum_{a\in\mathcal{A}} t_a(\bar{\boldsymbol{v}})\bar{v}_a && && (37)\\
\text{subject to} \quad & \sum_{a\in\mathcal{A}}\sum_{w\in\mathcal{W}} (t_a(\bar{\boldsymbol{v}}) - \varepsilon_a^w)(x_a^w - \bar{x}_a^w) \ge 0 && \forall \boldsymbol{x} \in \boldsymbol{X} && (38)\\
& \bar{v}_a^\kappa = \sum_{w\in\mathcal{W}} \bar{x}_a^w && \forall a \in \mathcal{A} && (39)\\
& \bar{x} \in \boldsymbol{X} && && (40)\\
& 0 \le \varepsilon_a^w \le \frac{\kappa}{1+\kappa} t_a(\bar{\boldsymbol{v}}) && \forall a \in \mathcal{A} && (41)
\end{aligned}
$$

Problem (37) is an instance of mathematical programs with equilibrium constraints (MPEC). We can replace the equilibrium condition (38) by the following KKT conditions to create a single-level optimization problem:

$$
\begin{aligned}
& t_a(\bar{\boldsymbol{v}}) - \varepsilon_a^w + \pi_i^w - \pi_j^w \ge 0 && \forall w \in \mathcal{W}, a \in \mathcal{A} && (42)\\
& \bar{x}_a^w(t_a(\bar{\boldsymbol{v}}) - \varepsilon_a^w + \pi_i^w - \pi_j^w) = 0 && \forall w \in \mathcal{W}, a \in \mathcal{A} && (43)\\
& \sum_{a\in\mathcal{A}_i^+} \bar{x}_a^w - \sum_{a\in\mathcal{A}_i^-} \bar{x}_a^w = q_i^w && \forall w \in \mathcal{W}, i \in \mathcal{N} && (44)
\end{aligned}
$$

The resulting problem is a mathematical program with complementarity conditions (MPCC), which is nonlinear and nonconvex. Finding a global solution to MPCC problems is in general difficult, and Kleer and Schäfer (2016) has shown that solving the above MPCC optimally is NP-hard. In order to solve this problem, we use an interior point method by utilizing the Ipopt nonlinear solver (Wächter and Biegler, 2006) with multiple starting solutions.

5.1 Numerical Experiments

In this section we present some examples to compare the total travel times in MSatUE and PRUE numerically for both separable and asymmetric networks. We approximate MSatUE by $\mathsf{UE\text{-}PE\text{-}}\boldsymbol{X}$ and solve it by the Ipopt nonlinear solver, after reformulating (36) as a single-level optimization problem using KKT conditions. We use the Julia Language and the JuMP package (Dunning et al., 2017) for modeling and interfacing with the Ipopt solver.

5.1.1 Simple Networks

To test the validity and the strength of $\mathsf{UE\text{-}PE\text{-}}\boldsymbol{X}$ model, we first consider Examples 1 and 2 in Figure 5. We compare PoSat under $\mathsf{UE\text{-}PE\text{-}}\boldsymbol{X}$ with the PoSat under MSatUE obtained in Section

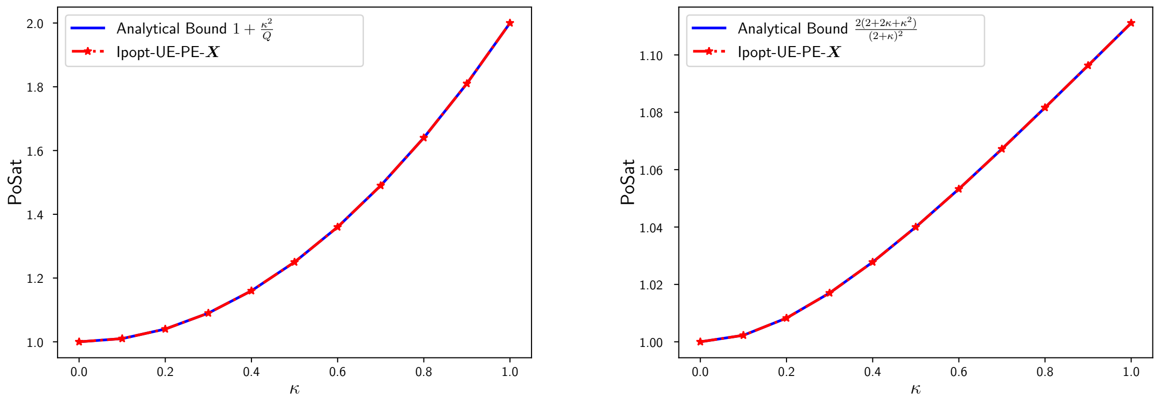

(a) Example 1 with $Q = 1$ (b) Example 2

Figure 5: PoSat for the simple networks in Figure 4

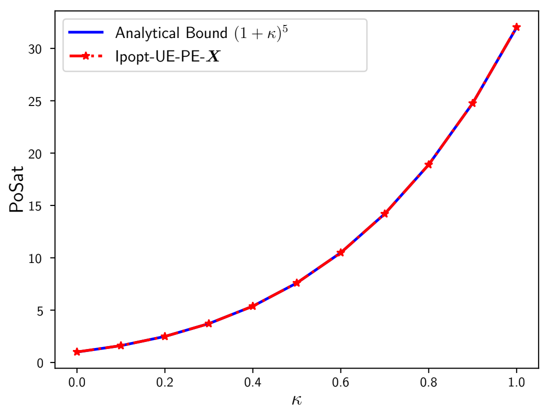

Figure 6: PoSat for the circular network in Figure 2

4.6. As it can be seen, we obtained identical results for both examples under UE-PE-$\boldsymbol{X}$, using Ipopt solver, which suggests that the UE-PE-$\boldsymbol{X}$ model is an effective model.

5.1.2 Circular Network of Christodoulou et al. (2011)

We also compute the PoSat under UE-PE-$\boldsymbol{X}$ model for the circular network of Christodoulou et al. (2011) presented in Figure 2. For numerical experiments, we assign m and l to the smallest positive integers such that $\frac{m}{l} = (1+\kappa)^5$, and $\kappa \in \{0, 0.1, 0.2, ..., 1\}$. We also set $n = 4$. As it can be seen, we obtained identical results for circular network under UE-PE-$\boldsymbol{X}$, using the Ipopt solver, which shows that the UE-PE-$\boldsymbol{X}$ model can obtain the upper bound provided in Lemma 5.

5.1.3 Larger Networks

We present some examples to compare the total travel times in MSatUE and PRUE numerically and compare the numerical worst-cases with the analytical bound given in Theorem 2 for larger networks with both separable and non-separable, asymmetric arc cost functions. As (36) is a non-convex problem, the Ipopt solver can produce a local minimum at best. To obtain a higher-quality local minimum, we solve the problem multiple times by using different initial solution. For generating different initial solutions for the network with separable arc cost functions, we utilize UE-PE-$\boldsymbol{V}$ model. We generate initial $\boldsymbol{\lambda}$ randomly and use the Frank-Wolfe algorithm to obtain the corresponding $\boldsymbol{v}$ and $\boldsymbol{x}$. For the network with non-separable cost function, we can use the fixed point method (Dafermos, 1980) with a randomized $\boldsymbol{\lambda}$ to obtain an initial solution $\boldsymbol{x}$. We randomly generate five initial starting points for each example and report the largest PoSat values.

We first consider the nine-node network presented in Hearn and Ramana (1998). The nine-node network consists of 9 nodes and 18 arcs, and the travel time functions are polynomials of order $n = 4$. We also create an asymmetric variant of the nine-node network as shown in Figure 9 in Appendix B. The asymmetric nine-node network has non-separable arc cost function in the form of (49). The comparison result is presented in Figure 7a. As Figure 7a represents PoSat_κ increases with κ for both symmetric and asymmetric nine-node network since PRUE total travel time is fixed with respect to κ, while the worst-case MSatUE total travel time increases as κ increases. Moreover, PoSat_κ is smaller for symmetric nine-node network compared to the asymmetric nine-node network for smaller κ values (0.1 and 0.2), but it is greater for larger κ values ($\kappa \geq 0.3$). In general, the gap between PoSat_κ for symmetric nine-node network and asymmetric nine-node network is small.

Figure 7b compares the numerical PoSat_κ with the analytical bound provided in Theorem 2 for MSatUE for the nine-node network. We observe that there is a large gap between the analytical and numerical bounds which increases with κ. Although the analytical result certainly provides a valid bound, it is too large to be practically useful in realistic road networks. This indicates opportunities for empirical studies on the analytical bounds that depend on more network-specific information such as travel demands and travel time functions. The bound $(1+\kappa)^{n+1}$ in Theorem 2 is independent from such network-specific information.

We also consider the Sioux Falls network presented in Suwansirikul et al. (1987), which consists of 24 nodes, 76 arcs, and 576 OD pairs. The arc travel cost function is the BPR function, which is a polynomial function with degree $n = 4$. We also consider an asymmetric variant of Sioux Falls network with arc cost function in the form of (49). As Figure 8a represents, PoSat_κ increases with κ for both symmetric and asymmetric Sioux Falls network, and it is greater compared to the nine-node network for both symmetric and asymmetric networks. Furthermore, PoSat_κ is greater for asymmetric Sioux Falls network compared with the symmetric Sioux Falls network for all positive κ values, and the gap between PoSat_κ for symmetric Sioux Falls network and PoSat_κ for asymmetric Sioux Falls network increases with κ. Figure 8b compares the numerical PoSat_κ with the analytical bound. The gap between the analytical and the numerical bound is tighter compared to the nine-node network, but it is still considerable.

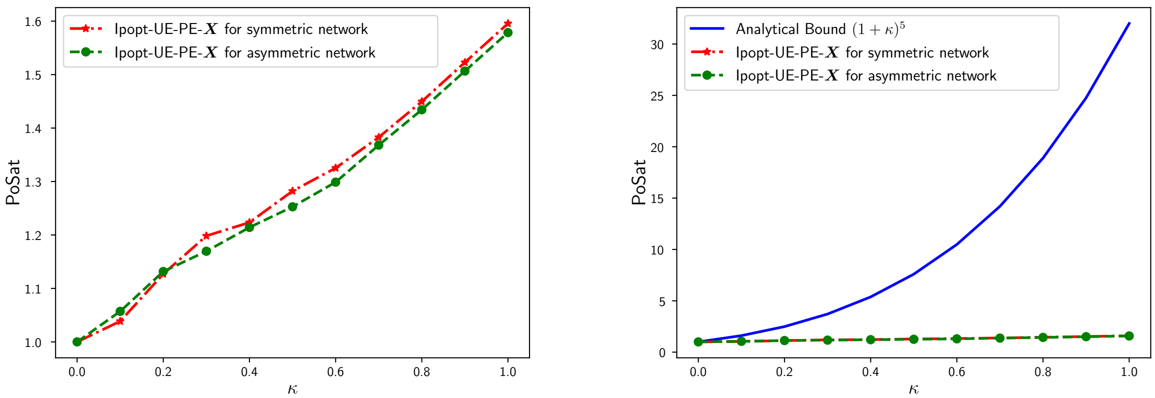

(a) Approximate PoSat (Ipopt-UE-PE-$\boldsymbol{X}$) (b) Comparing analytical and numerical PoSat

Figure 7: PoSat for nine-node network

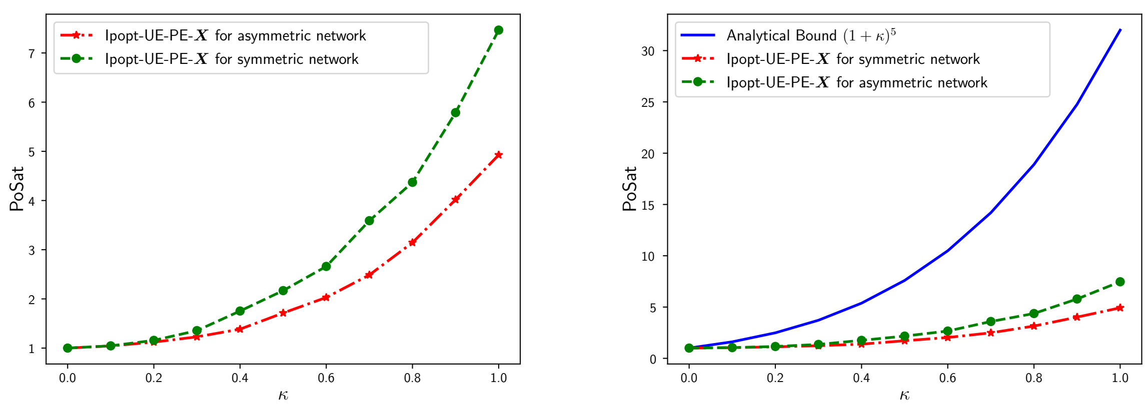

(a) Approximate PoSat (Ipopt-UE-PE-$\boldsymbol{X}$) (b) Comparing analytical and numerical PoSat

Figure 8: PoSat for Sioux Falls network

6 Concluding Remarks

When network users are satisficing decision makers, the resulting satisficing user equilibria may degrade the system performance, compared to the perfectly rational user equilibrium. To quantify how much the performance can deteriorate, this paper has quantified the worst-case analytical bound on the price of satisficing. We also quantified the price of satisficing for several networks numerically and compare it to the analytical bound.

We suggest potential future research directions to improve the results of this paper. For the proposed analytical bound, our result is based on the condition (33). By attempting to relax this condition, one may obtain a global bound for any value of κ. One may also try to develop analytical bounds that depend on more network-specific information such as travel demands and travel time functions.

In deriving the analytical bound, we utilized a novel technique comparing equilibrium patterns before and after the travel demand is increased; namely $\boldsymbol{V}$ and $\boldsymbol{V}_{1+\kappa}$. Applying this technique in the context of the price of risk aversion and the deviation ratio would be an interesting research direction.

Acknowledgments

This research was partially supported by the National Science Foundation under grant CMMI-1351357. The authors are thankful for the anonymous reviewers whose constructive comments have greatly improved this manuscript.

References

Beckmann, M., C. McGuire, C. Winsten. 1956. *Studies in the Economics of Transportation*. Yale University Press, New Haven, Conn.

Brown, D. B., M. Sim. 2009. Satisficing Measures for Analysis of Risky Positions. *Management Science* **55**(1) 71–84.

Charnes, A., W. W. Cooper. 1963. Deterministic equivalents for optimizing and satisficing under chance constraints. *Operations Research* **11**(1) 18–39.

Chen, H.-C., J. W. Friedman, J.-F. Thisse. 1997. Boundedly rational Nash equilibrium: a probabilistic choice approach. *Games and Economic Behavior* **18**(1) 32–54.

Christodoulou, G., E. Koutsoupias, P. G. Spirakis. 2011. On the performance of approximate equilibria in congestion games. *Algorithmica* **61**(1) 116–140.

Dafermos, S. 1980. Traffic equilibrium and variational inequalities. *Transportation Science* **14**(1) 42–54.

Dafermos, S., A. Nagurney. 1984. Sensitivity analysis for the asymmetric network equilibrium problem. *Mathematical Programming* **28**(2) 174–184.

de Palma, A., Y. Nesterov. 1998. Optimization formulations and static equilibrium in congested transportation networks. *CORE Discussion Paper 9861, Université Catholique de Louvain, Louvain-la-Neuve*. 12–17.

Di, X., X. He, X. Guo, H. X. Liu. 2014. Braess paradox under the boundedly rational user equilibria. *Transportation Research Part B: Methodological* **67** 86–108.

Di, X., H. X. Liu. 2016. Boundedly rational route choice behavior: A review of models and methodologies. *Transportation Research Part B: Methodological* **85** 142–179.

Di, X., H. X. Liu, J.-S. Pang, X. J. Ban. 2013. Boundedly rational user equilibria (BRUE): Mathematical formulation and solution sets. *Transportation Research Part B: Methodological* **57** 300–313.

Dunning, I., J. Huchette, M. Lubin. 2017. JuMP: A modeling language for mathematical optimization. *SIAM Review* **59**(2) 295–320. doi: 10.1137/15M1020575.

Englert, M., T. Franke, L. Olbrich. 2010. Sensitivity of Wardrop equilibria. *Theory of Computing Systems* **47**(1) 3–14.

Friesz, T. L., D. Bernstein. 2016. *Foundations of network optimization and games*. Springer.

Ge, Y., X. Zhou. 2012. An alternative definition of dynamic user optimum on signalised road networks. *Journal of Advanced Transportation* **46**(3) 236–253.

Guo, X. 2013. Toll sequence operation to realize target flow pattern under bounded rationality. *Transportation Research Part B: Methodological* **56** 203–216.

Han, K., W. Szeto, T. L. Friesz. 2015. Formulation, existence, and computation of boundedly rational dynamic user equilibrium with fixed or endogenous user tolerance. *Transportation Research Part B: Methodological* **79** 16 – 49. doi: http://dx.doi.org/10.1016/j.trb.2015.05.002. URL `http://www.sciencedirect.com/science/article/pii/S0191261515000971`.

Hearn, D. W., M. V. Ramana. 1998. Solving congestion toll pricing models. *Equilibrium and Advanced Transportation Modelling*. Springer, 109–124.

Jaillet, P., S. D. Jena, T. S. Ng, M. Sim. 2016. Satisficing awakens: Models to mitigate uncertainty. *Working Paper* URL `http://www.optimization-online.org/DB_HTML/2016/01/5310.html`.

Kleer, P., G. Schäfer. 2016. The impact of worst-case deviations in non-atomic network routing games. *International Symposium on Algorithmic Game Theory*. Springer, 129–140.

Koutsoupias, E., C. Papadimitriou. 1999. Worst-case equilibria. *Annual Symposium on Theoretical Aspects of Computer Science*. Springer, 404–413.

Lam, S.-W., T. S. Ng, M. Sim, J.-H. Song. 2013. Multiple objectives satisficing under uncertainty. *Operations Research* **61**(1) 214–227.

Lou, Y., Y. Yin, S. Lawphongpanich. 2010. Robust congestion pricing under boundedly rational user equilibrium. *Transportation Research Part B: Methodological* **44**(1) 15–28.

Mahmassani, H. S., G.-L. Chang. 1987. On boundedly rational user equilibrium in transportation systems. *Transportation Science* **21**(2) 89–99.

Meng, Q., Z. Liu, S. Wang. 2014. Asymmetric stochastic user equilibrium problem with elastic demand and link capacity constraints. *Transportmetrica A: Transport Science* **10**(4) 304–326.

Nakayama, S., R. Kitamura, S. Fujii. 2001. Drivers' route choice rules and network behavior: Do drivers become rational and homogeneous through learning? *Transportation Research Record: Journal of the Transportation Research Board* **1752**(1) 62–68.

Nikolova, E., N. E. Stier-Moses. 2015. The burden of risk aversion in mean-risk selfish routing. *Proceedings of the Sixteenth ACM Conference on Economics and Computation*. ACM, 489–506.

Panicucci, B., M. Pappalardo, M. Passacantando. 2007. A path-based double projection method for solving the asymmetric traffic network equilibrium problem. *Optimization Letters* **1**(2) 171–185.

Patriksson, M. 2015. *The traffic assignment problem: models and methods*. Courier Dover Publications.

Perakis, G. 2007. The "price of anarchy" under nonlinear and asymmetric costs. *Mathematics of Operations Research* **32**(3) 614–628.

Roughgarden, T., É. Tardos. 2002. How bad is selfish routing? *Journal of the ACM (JACM)* **49**(2) 236–259.

Sheffi, Y. 1985. *Urban transportation networks: equilibrium analysis with mathematical programming methods*.

Simon, H. A. 1955. A behavioral model of rational choice. *The Quarterly Journal of Economics* 99–118.

Simon, H. A. 1956. Rational choice and the structure of the environment. *Psychological Review* **63**(2) 129.

Smith, M. J. 1979. The existence, uniqueness and stability of traffic equilibria. *Transportation Research Part B: Methodological* **13**(4) 295–304.

Sun, L., M. H. Karwan, C. Kwon. 2018. Generalized bounded rationality and robust multi-commodity network design. *Operations Research* **66**(1) 42–57.

Suwansirikul, C., T. L. Friesz, R. L. Tobin. 1987. Equilibrium decomposed optimization: a heuristic for the continuous equilibrium network design problem. *Transportation Science* **21**(4) 254–263.

Szeto, W., H. K. Lo. 2006. Dynamic traffic assignment: properties and extensions. *Transportmetrica* **2**(1) 31–52.

Takalloo, M., C. Kwon. 2018. Sensitivity of Wardrop equilibria: revisited. *Working Paper* URL `http://www.chkwon.net/papers/takalloo_sensitivity.pdf`.

Wächter, A., L. T. Biegler. 2006. On the implementation of an interior-point filter line-search algorithm for large-scale nonlinear programming. *Mathematical Programming* **106**(1) 25–57.

Wu, J., H. Sun, D. Z. Wang, M. Zhong, L. Han, Z. Gao. 2013. Bounded-rationality based day-to-day evolution model for travel behavior analysis of urban railway network. *Transportation Research Part C: Emerging Technologies* **31** 73–82.

Xu, H., H. Yang, J. Zhou, Y. Yin. 2017. A route choice model with context-dependent value of time. *Transportation Science* **51**(2) 536–548.

Ye, H., H. Yang. 2017. Rational behavior adjustment process with boundedly rational user equilibrium. *Transportation Science* **51**(3) 968–980.

Zhu, S., D. Levinson. 2010. Do people use the shortest path? An empirical test of Wardrop's first principle. *91th Annual Meeting of the Transportation Research Board, Washington*, vol. 8.

Appendices

A Proof of Lemma 7

Proof of Lemma 7. This is a minor variant to the proof of Englert et al. (2010, Theorem 3). Since $\boldsymbol{v}^0 \in \boldsymbol{F}$ and $\widehat{\boldsymbol{v}}^0 \in \boldsymbol{F}_{1+\kappa}$ are PRUE flows that minimize $\Phi(\cdot)$ over their corresponding feasible sets, we have

$$\Phi(\boldsymbol{v}^0) \le \Phi\Big(\frac{\widehat{\boldsymbol{v}}^0}{1+\kappa}\Big) \quad \text{and} \quad \Phi(\widehat{\boldsymbol{v}}^0) \le \Phi\big((1+\kappa)\boldsymbol{v}^0\big),$$

which imply

$$(1+\kappa)^{n+1} \sum_{a\in\mathcal{A}} \frac{b_a}{n+1} (v_a^0)^{n+1} \le \sum_{a\in\mathcal{A}} \frac{b_a}{n+1} (\widehat{v}_a^0)^{n+1} \tag{45}$$

and

$$\sum_{a\in\mathcal{A}} \frac{b_a}{n+1} (\widehat{v}_a^0)^{n+1} \le (1+\kappa)^{n+1} \sum_{a\in\mathcal{A}} \frac{b_a}{n+1} (v_a^0)^{n+1} \tag{46}$$

respectively.

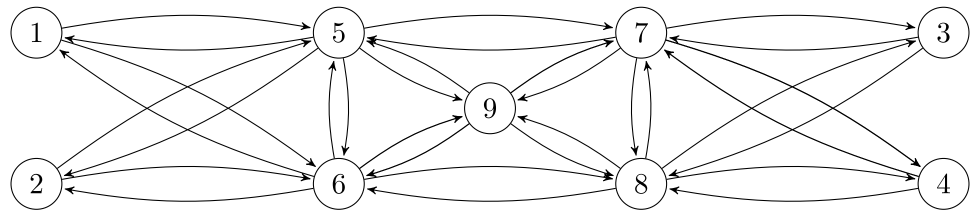

Figure 9: Asymmetric nine-node network

Let us assume that $C(\widehat{\boldsymbol{f}}^0) > (1+\kappa)^{n+1} C(\boldsymbol{f}^0)$, which is equivalent to

$$(1+\kappa)^{n+1} \sum_{a \in \mathcal{A}} b_a (v_a^0)^{n+1} < \sum_{a \in \mathcal{A}} b_a (\widehat{v}_a^0)^{n+1}. \tag{47}$$

From $n \times (45) + ((n+1)(1+\kappa)^n - 1) \times (46) + ((1+\kappa)^n - 1) \times (47)$, we obtain

$$\theta_1 \sum_{a \in \mathcal{A}} \frac{b_a (v_a^0)^{n+1}}{n+1} < \theta_2 \sum_{a \in \mathcal{A}} \frac{b_a (\widehat{v}_a^0)^{n+1}}{n+1} \tag{48}$$

where

$$\theta_1 = n \cdot \frac{(1+\kappa)^{n+1}}{n+1} - ((n+1)(1+\kappa)^n - 1) \cdot \frac{(1+\kappa)^{n+1}}{n+1} + ((1+\kappa)^n - 1) \cdot (1+\kappa)^{n+1} = 0$$
$$\theta_2 = n \cdot \frac{1}{n+1} - ((n+1)(1+\kappa)^n - 1) \cdot \frac{1}{n+1} + ((1+\kappa)^n - 1) = 0$$

for all $\kappa \geq 0$. Therefore, (48) leads to $0 < 0$, which is a contradiction. We conclude that $C(\widehat{\boldsymbol{f}}^0) \leq (1+\kappa)^{n+1} C(\boldsymbol{f}^0)$. □

B Nine-node Asymmetric Networks

In order to test the performance of UE-PE-$\boldsymbol{X}$ model in an asymmetric network, we create an asymmetric version of the nine-node network considered by Hearn and Ramana (1998). In the asymmetric nine-node network, which has been shown in Figure 9, we add a few additional arcs and assume that the arc travel cost function is:

$$t_a(\boldsymbol{v}) = A_a + B_a \left(\frac{0.5 v_{\widehat{a}} + v_a}{C_a} \right)^4 \tag{49}$$

where $\widehat{a}$ is the flow in the opposite arc. Thus, the arc travel function depends not only on the flow in that arc, but also on the flow in the arc in opposite direction. The values of parameters A_a, B_a and C_a are given in Table 1 for each arc.

Table 1: asymmetric nine-node network arc cost function parameters

a	A_a	B_a	C_a
(1,5)	12	1.80	5
(1,6)	18	2.70	6
(2,5)	35	5.25	3
(2,6)	35	5.25	9
(5,6)	20	3.00	9
(5,7)	11	1.65	2
(5,9)	26	3.90	8
(6,8)	33	4.95	6
(6,9)	30	4.50	8
(7,3)	25	3.75	3
(7,4)	24	3.60	6
(7,8)	19	2.85	2
(8,3)	39	5.85	8
(8,4)	43	6.45	6
(9,7)	26	3.90	4
(9,8)	30	4.50	8
(5,1)	12	1.80	5
(6,1)	18	2.70	6
(5,2)	35	5.25	3
(6,2)	35	5.25	9
(6,5)	20	3.00	9
(7,5)	11	1.65	2
(9,5)	26	3.90	8
(8,6)	33	4.95	6
(9,6)	30	4.50	8
(3,7)	25	3.75	3
(4,7)	24	3.60	6
(8,7)	19	2.85	2
(3,8)	39	5.85	8
(4,8)	43	6.45	6
(7,9)	26	3.90	4
(8,9)	30	4.50	8